# INFLAMMATION IN THE EARLY PATHOGENESIS OF DIABETIC RETINOPATHY

by

**Shukun Wang**

**A Thesis**

*Submitted to the Faculty of Purdue University*

*In Partial Fulfillment of the Requirements for the degree of*

**Master of Science**


Department of Biological Sciences

Indianapolis, Indiana

August 2018

# THE PURDUE UNIVERSITY GRADUATE SCHOOL
# STATEMENT OF COMMITTEE APPROVAL

Dr. Teri Belecky-Adams, Chair
Department of Biology
Dr. Denise Slayback-Barry
Department of Biology
Dr. Guoli Dai
Department of Biology

**Approved by:**
Dr. James Marrs
Head of the Graduate Progrm

# ACKNOWLEDGEMENTS

I would like to thank my advisor, Dr. Belecky-Adams, for her guidance and encouragement. Dr. Belecky-Adams allowed me to work on my own but also steered me in the right direction whenever I needed it. Dr. Belecky-Adams was always there whenever I needed her help. I would also thank my committee members Dr. Dai and Dr. Slayback-Barry. They helped guide my understanding of my field while also broadening my research. I would like to thank Dr. Baucum for his help in progressing my research. I am grateful to the School of Science at IUPUI and Biology Department for their help in providing me with the resources to complete my project. I would also like to thank my predecessors Dr. Dharmarajan and Dr. Wilson for their contributions to my project. Finally, I would like to express my profound gratitude to my family for their continuous encourage and support throughout my years of study. Thank you.

# TABLE OF CONTENTS

# LIST OF TABLES

# LIST OF FIGURES

# LIST OF ABBREVIATIONS

- ADA– American Diabetes Association
- AGE's – Advanced glycation end products
- AIF or IBA – Allograft Inflammatory Factor
- AKITA or AK – $Ins^{Akita}$
- AKT – AKR Mouse Transforming
- ANOVA – One-Way Analysis of Variance
- ARAF or MNK – Serine/Threonine Protein Kinase
- B2M – β -2 Microglobulin
- BAD – BCL-2-Associated Death Promoter
- BCL-2 – B-Cell Lymphoma 2
- BIM – BCL-2-Like Protein 11
- BRB – Blood-Retinal Barrier
- CCL – Chemokine Ligand
- CCL2 – Chemokine (C-C) Ligand
- CD – Cluster of Differentiation
- CHC22- Clathrin Heavy Chain on Chromosome 22
- CNS – Central Nervous System
- CRP – C Reactive Protein
- CSF – Colony Stimulating Factor
- DAG – Diaglycerol
- DB or db/db – $Lepr^{DB}$
- DNA-PK – DNA-Dependent Protein Kinase
- DR – Diabetic Retinopathy
- ECM – Extracellular Matrix
- EGFR – Epidermal Growth Factor
- ELK-1 – ETS Domain Containing Protein
- ER – Endoplasmic Reticulum
- ERK – Extracellular Signal-Regulated Kinases
- FOXO – Forkhead Box O
- GEF – Guanine Nucelotide Exchange Factor
- GFAP – Glial Fibrillary Acid Protein
- GLAST – Glutamine Aspartate Transporter
- GM-CSF – Granulocyte Macrophage Colony Stimulating Factor
- GRB2 – Growth Factor Receptor Bound Protein 2
- Gs – Glutamine Synthetase
- GSK3 – Glycogen Synthase Kinase 3
- HDAC6 – Histone Deacetylase 6
- IAP – Inhibitor of Apoptosis
- IB4 – Isolectin B4

- IFN – Interferon
- IFN-Y – Interferon-γ
- IL – Interleukin
- IRF – Interferon-Regulating Factor
- IRMA – Intraretinal Microvascular Abnormality
- JAK – Janus Kinase
- JNK – C-JUN N-Terminal Kinase
- MAP3K – MAP Kinase Kinase Kinase
- MAPK – Mitogen Activated Protein Kinase
- MCL-1 – Induced Myeloid Leukemia Cell Differentiation Protein
- MEK – Mitogen Activated Protein Kinase Kinase
- MHC – Major Histocompatibility Complex
- MMP – Matrix Metalloproteinase
- MSK – Stress Activated Protein Kinase
- mTORC2 – Mammalian Target of Rapamycin complex 2
- NCAN – Neurocan Core Protein
- NG2 – Neural/Glial Antigen 2
- NK – Natural Killer cells
- NF-κB – Nuclear Factor Kappa-Light-Chain Enhancer of Activated B Cells
- pAKT – Phosphorylated AKT
- PBB – PDGF-BB
- PCAN – Phosphacan
- PCNA – Proliferating Nuclear Antigen
- PDGF – Platelet-Derived Growth Factor
- PDGF-BB – Platelet-Derived Growth Factor Homodimer BB
- PDGFRβ – Platelet-Derived Growth Factor Receptor β
- PDR – Proliferative Diabetic Retinopathy
- pERK – Phosphorylated ERK
- PHLPP – H Domain and Leucine-Rich Repeat Protein Phosphatase
- PI3K – Phosphoinositide 3-Kinase
- $PIP_2$ – Phosphatidylinositol 4,5 Bisphosphate
- $PIP_3$ – Phosphatidylinositol 3,4,5-Triphosphate
- PKC – Protein Kinase C
- PLA2 – Phospholipase A2
- PP2A – Protein Phosphatase 2A
- pPDGFRβ – Phosphorylated PDGFRβ
- PRR – Pattern Recognition Receptor
- PtdIns – Phosphatidylinositol
- PTEN – Phosphatase and Tensin Homolog

- PVDF – Polyvinylidene Fluoride
- RAF – Rapidly Accelerated Fibrosarcoma
- RAF1 or CRAF – RAF-1 Proto-Oncogene
- RAGE – Receptor for Advanced Glycation End Products
- RANTES – Regulated on Activation, Normal T Cell Expressed and Secreted
- ROS – Reactive Oxygen Species
- RPE – Retinal Pigmented Epithelium
- RSK – Ribosomal S6 Kinase
- RT-qPCR – Reverse-Transcriptase Quantitative Polymerase Chain Reaction
- S100 – S100 Calcium Protein-Binding B
- SDHA – Succinate Dehydrogenase Complex Subunit A
- SH2 – SRC Homology 2
- SH3 – SRC Homology 3
- SHP-1 OR SHIP-1 – SRC Homology Domain 2 Containing Inositol-5-Phosphatase
- SOX2 – Sex Determining Region Y (SRY) – Box2
- SPRY – Sprouty
- SRP14 – Signal Recognition Particle 14 kDa
- STAT – Signal Transducer and Activator of Transcription Protein
- TGF – Transforming Growth Factor
- TGF-β – Transforming Growth Factor β
- TH1 – Helper Type 1 Thymus Cell
- TH2 – Helper Type 2 Thymus Cell
- THBS – Thrombospondin
- TIMP – Tissue Inhibitor of Metalloproteinase
- TLR – Toll-Like Receptor
- TNF – Tumor Necrosis Factor
- TSC2 – Tuberous Sclerosis Protein 2
- VEGF – Vascular Endothelial Growth Factor
- VIM – Vimentin
- WHO – World Health Organization
- WT – Wild type or C57BL/6

# ABSTRACT

Author: Wang, Shukun. MS
Institution: Purdue University
Degree Received: August 2018
Title: Inflammation in the Early Pathogenesis of Diabetic Retinopathy
Major Professor: Teri Belecky-Adams

**Introduction –** Diabetes is a growing health concern. Diabetic retinopathy (DR), is a complication resulting from long-term diabetes and is currently the leading cause of blindness in the US. The cause of pericyte loss, an early indiciator of DR progression, is currently unknown. Inflammation, increased in diabetes, could play a role in the progression of DR and be one of the causes of pericyte loss.

**Methods and Materials-** Retinas from 3, 6, 12, 18, and 24 week Akita (AK) and DB mice were taken and cell counts, vasculature, and mRNA expression were examined. Pericytes treated with IFN-γ and PDGF-BB in chronic and acute conditions and PDGFRβ signaling was determined using Western blot analysis. Apoptosis and proliferation were examined using western blots and immunohistochemistry of IFN-γ treated pericytes.

**Results-** Pericytes numbers were changed as 3 weeks in DB and Akita models. Proinflammatory markers increased at 6 weeks and displayed their maximum expression at 12 and 18 weeks. Chronic treatments with IFN-γ changed AKT and PKCδ activation and increases pericytes apoptosis.

**Discussion-** Pericyte loss appears to begin prior to an increase in pro-inflammatory factors indicating that perhaps retinal inflammtion may not initiate pericyte loss or that loss of pericyte numbers at 3 weeks may be due to reduced numbers of neural crest cells migrating to vasculature or a reduced number of neural crest cells differentiating into pericytes. Proinflammatory changes occur between 3-6 weeks in both Akita and DB models of diabetes; however, the peak levels in expression of proinflammtory markers differs between Akita and DB models.

One of the markers that increased very early in the progression of diabetic retinopathy, IFN-γ, triggered apoptosis in isolated retinal pericytes by increasing protein kinase Cδ activation, which then reduced activity of AKT.

# 1. INTRODUCTION

## 1.1 Diabetes

Diabetes is a prevalent and growing health concern in the United States and across the world. As of 2014, 30.3 million Americans and 422 million people worldwide have diabetes (American Diabetes Association, World Health Organization, 2017). Of those 30.3 million people (9.4% of US population), 23.1 million are diagnosed with about 7.2 million people being undiagnosed (ADA, 2017). It is estimated that 5% of those have type 1 diabetes and around 90-95% of all diabetics are type 2 (ADA, 2017). In the world, the rate of diabetes has currently doubled from 4.7% in 1980 to 8.5% in 2014 (WHO, 2017). It is said globally that 1.6 million deaths can be directly linked to diabetes and 2.2 million can be linked indirectly to high blood glucose (WHO, 2017).

Hyperglycemia, an excessive amount of blood glucose, is one of the major characteristics of diabetes. Hyperglycemia is the result of a loss of insulin production, secretion, insulin resistance, or a combination of all three (ADA, 2017). There are two main types of diabetes, type 1 and type 2. Type 1, also known as insulin-dependent and formerly juvenile-onset diabetes, is an autoimmune condition in which the immune system attacks the pancreatic beta cells leading to a loss in insulin production (CDC, 2011). Type 2, formerly known as adult-onset, is often attributed to insulin resistance, low insulin production, or a combination of both (CDC, 2011). Insulin resistance is when the cells in the body do not respond to the insulin produced, often leading to an overproduction of insulin. A third smaller type of diabetes is gestational diabetes in which 2-10% pregnant mothers have high blood sugar (CDC, 2011). This can cause development of type 2 diabetes later in life of both the child and the mother. One of the complications of diabetes is diabetic retinopathy (DR). It is currently the leading cause of

blindness in American adults, with around 9 million Americans over the age of 40 suffering from DR and related diseases (Saadine, 2008). In order to discuss the effect of diabetes on the eye, basic information concerning the eye will be introduced in the next section.

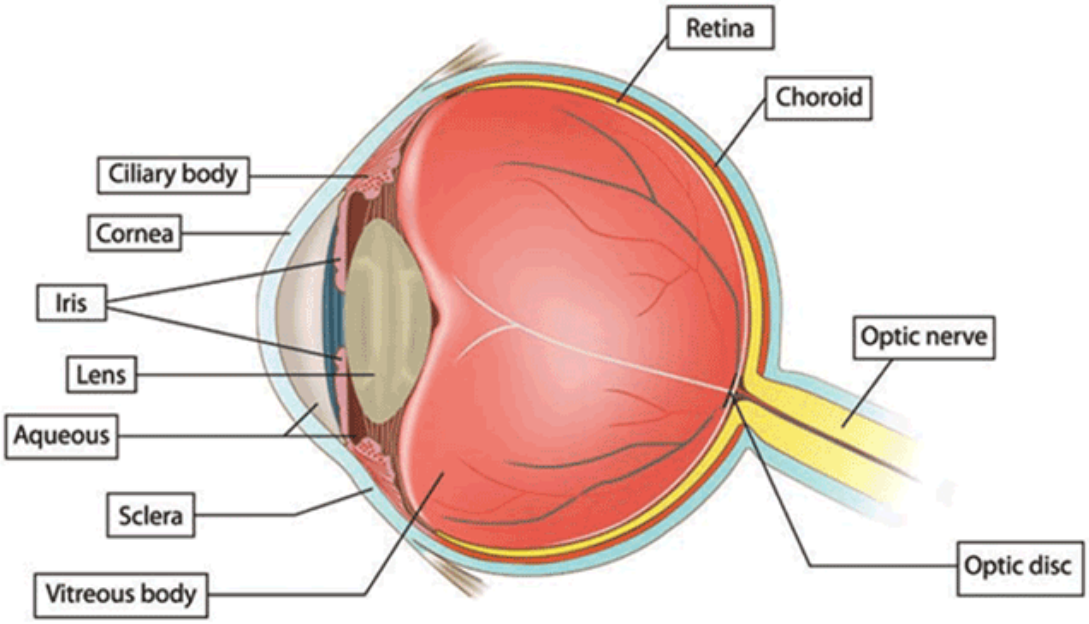


Figure 1 Image of major eye structures. Image from Glaucoma Research Foundation. (Eye Anatomy, 2017)

### 1.2 Retina and Eye

As shown in Figure 1, the affected area in patients suffering from DR lies in the retinal area, located in the back of the eye. The function of the eye is to convert light into signals for the brain to produce images and pictures. The retina contains photoreceptors that transform light into electrochemical impulses.

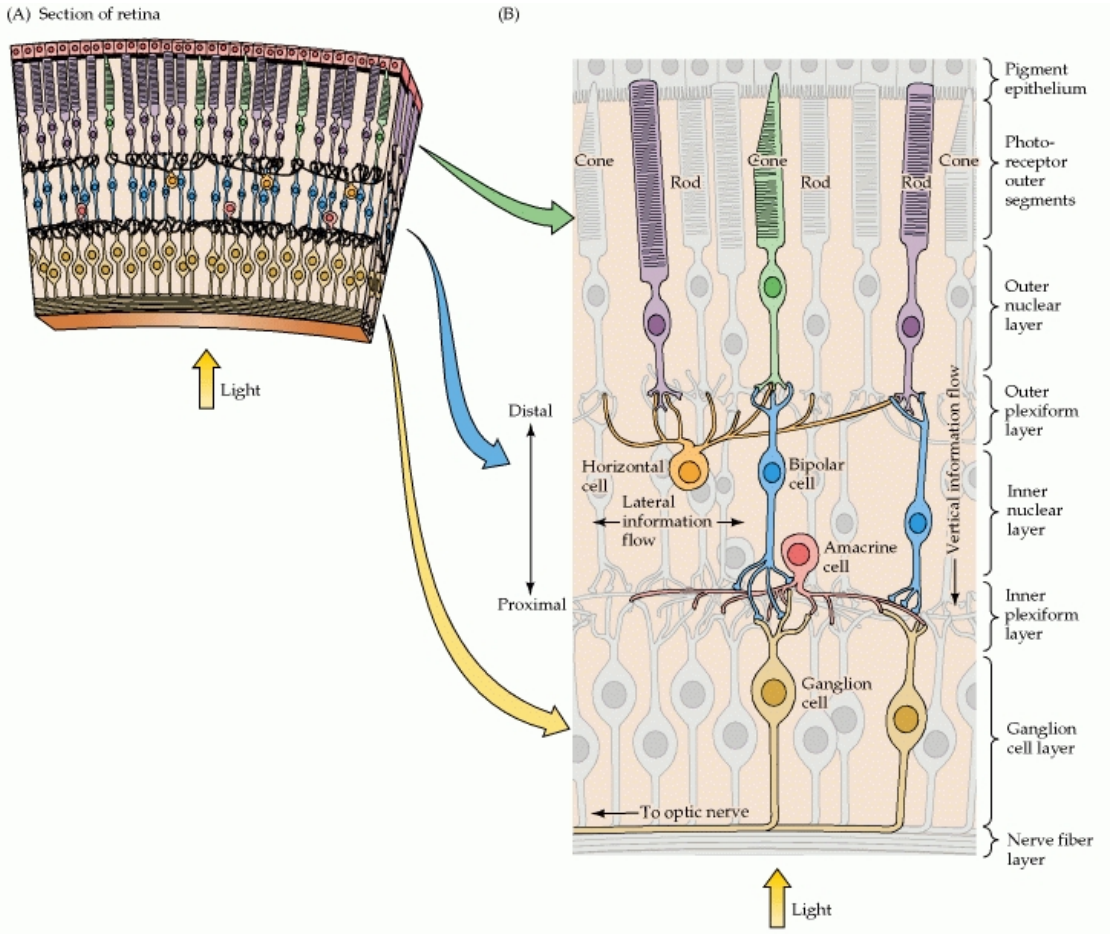


Figure 2 Light transmission in the retina. The 6 retinal layers along with information processing cells. Image from Purves et al., 2001.

Light is absorbed by the rods and cones in the photoreceptor layer, as shown in Figure 2 (Purves et al., 2001). Following phototransduction, neurotransmitter is released onto the bipolar cells (and some horizontal cells) (Purves et al., 2001). These bipolar cells transfer information through graded potentials to the ganglion cells (Purves et al., 2001). The ganglion cells, whose

axons form the optic nerve along with glial cells, send vital information directly to the other areas of the central nervous system (CNS) (Purves et al., 2001). Amacrine and horizontal cells are mostly used for lateral inhibition (Purvers et al., 2001). The horizontal cell helps integrate and regulate information from multiple photoreceptors to the bipolar cells while amacrine cells do the same for the ganglion cells (Masland, 2012). However, these are not the only cell types located in the retina.

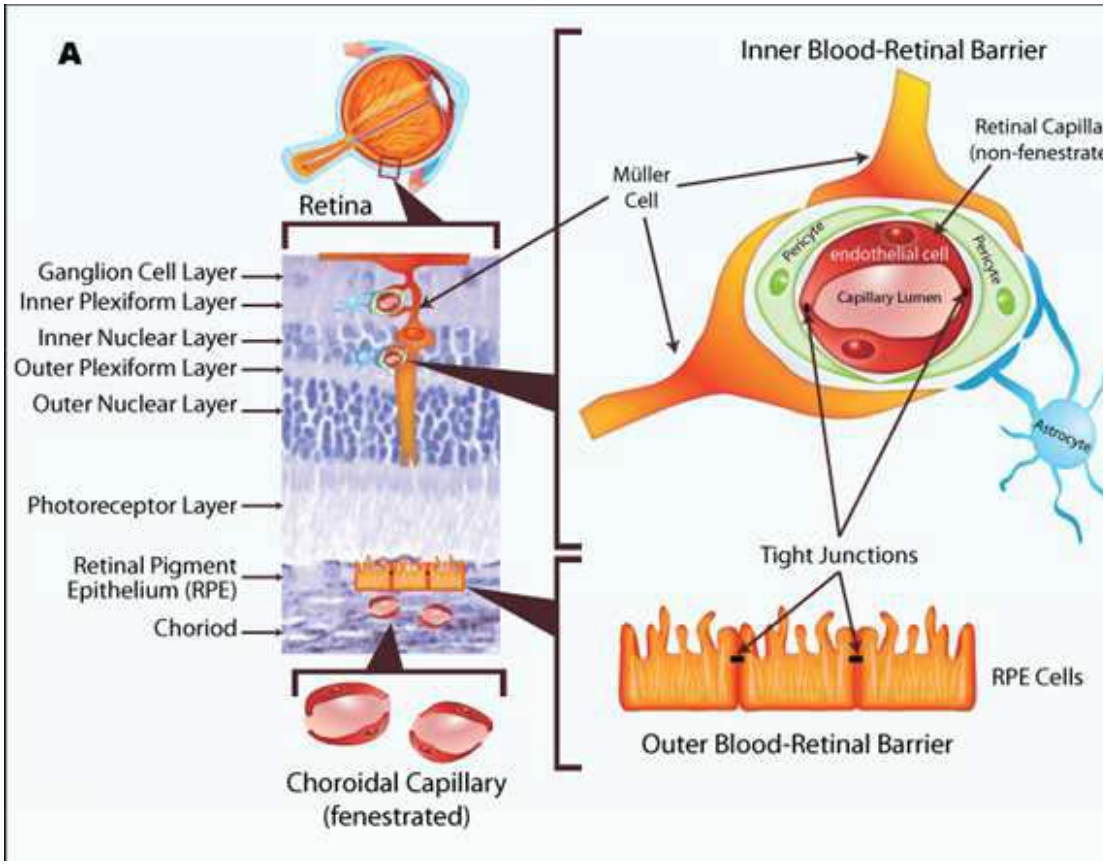


Figure 3 The location of retina within the eye. The 6 different retinal layers. Also, the location of blood-retinal barriers and how the barriers are perceived. Image from Kaur et al., 2008.

As shown in Figure 3, the retina contains six layers with the two blood-retinal barriers (BRBs). The BRB is a tight barrier that regulates ions, protein, and water flux inside and outside the retina (Cunha-Vaz et al., 2011). The outer blood-retinal barrier (oBRB) is made up of tight junctions from retinal pigmented epithelium (RPE) while the inner BRB (iBRB) is made up

of tight junctions between endothelial cells. Some of the important cells types besides the neurons and endothelial cells are the Mϋller glial, astrocytes, pericytes, and microglia. The Mϋller glia cell bodies are located in the inner nuclear layer, but they project their cellular processes through much of the other retinal layers, while the retinal astrocytes are located in the nerve fiber layer and their processes in the ganglion cell layer. The macroglia, which includes astrocytes and Mϋller glia, act as support cells and their main functions are maintaining homeostasis and providing structural support (Hoz et al., 2016). The microglia are located within the plexiform and nerve fiber layers and the microglia project their processes throughout the entire retina. The microglia act as the innate immune cells of the central nervous system (CNS).

The role of the endothelial cells is to form the vasculature of the retina while the pericytes are important in helping maintain the vasculature by acting as the support cells for the endothelial cells (Bergers and Song, 2005). These cells all communicate with each other to keep homeostasis inside the retina. Endothelial cells release platelet-derived growth factor homodimer subunit BB (PDGF-BB) which is important for the attraction and survival of pericytes. Pericytes, likewise, release transforming growth factor beta (TGF-β) which is important for iBRB maintenance and endothelial cell survival.

### 1.3 Diabetic Retinopathy Stages

There are 4 different stages which, in order of increasing intensity, are mild nonproliferative DR, moderate nonproliferative DR, severe nonproliferative DR, and proliferative diabetic retinopathy (PDR) (Wilkinson et al., 2003). In the mild nonproliferative DR, pericyte loss leads to endothelial cell loss and areas of swellings (microaneurysms), which can then lead to fluid leakage and eventually fluid buildup within the retina (macular edema) (Wilkinson et al., 2003). In the moderate nonproliferative DR, there is the addition of bleeding in the eye (intraretinal hemorrhaging), neuronal loss, inflammation, gliosis, dead cell debris buildup (cotton wool spots), and lipid buildup from leaky blood vessels (hard exudates) (Wilkinson et al., 2003). In the severe stage, there is the addition of formation of intraretinal microvascular abnormality (IRMA's) and the weakening of the blood vessel walls (venous beading) (Wilkinson et al., 2003). In PDR, the hallmark of development is the formation of new, leaky blood vessels that can eventually lead to blindness (Wilkinson et al., 2003).

It is estimated that 35.4% of all diabetic patients worldwide get some form of DR while 7.24% eventually develop PDR (Yau et al., 2012). There are also differences in the occurrence of DR between type 1 and type 2 as 77% of all type 1 develop DR while only 25% of type 2 get DR (Yau et al, 2012). This is magnified by the duration of diabetes as 86% of all type 1 diabetics with over 20 years of having diabetes develop DR while only 52% of all type 2 diabetics get DR with the same length of time (Yau et al., 2012). Type 1 diabetics that have diabetes over 20 years have 40.36% chance of getting PDR, while type 2 diabetics with over 20 years of diabetes only have a 15.13% chance of getting PDR (Yau et al., 2012). This could be due to differences in blood pressure, diabetes duration, and cause of disease. In order to study differences between the two types of diabetes, there are two main mouse models.

### 1.4 Diabetic Mouse Models

This study employs two different mouse models to emulate the two different diabetes types $Ins2^{Akita}$ (AK or Akita) and the $Lepr^{db}$(db/db or DB) model. The diabetes that develops in Akita mice is similar to type 1 diabetes in humans, while the homozygous DB mice develop diabetes that is similar to type 2 diabetes in humans (Robinson et al., 2012). The Akita mice have a missense mutation in the insulin 2 gene that results in pancreatic beta-cell toxicity and dysfunction (Wang et al., 1999). A mutation in the leptin receptor gene which results in a dysfunction in signaling to the hypothalamus, resulting in obesity, mild diabetes, islet hyperplasia, and hyperinsulinemia in the DB mice (Coleman, 1978). Both models are maintained on a C57BL/6J background (WT). As is the case with the different types of DR, the two mouse models have different progression of diabetes and DR.

The Akita mice are not obese and the disease develops due to an autosomal dominant trait. The Akita mice develop hyperglycemia and hypoinsulinemia around 4 to 6 weeks of age along with extreme thirst (polydipsia) and extreme urination (polyuria) (Yoshioka et al, 1997; Katsuda et al, 2013). Around 6 months there is increased albumin excretion and glomerular hypertrophy (Katsuda et al, 2013). The hyperglycemia can also cause oxidative stress and kidney injury in these animals (Ueno et al, 2002). At 4 months of age, the Akita mice display increased vascular permeability (Barber et al., 2005). Around 6 months of age the Akita mice develop the early retinal abnormalities like vascular leakages, decreased retinal blood flow, and pericyte loss while are 9 months there are symptoms like microaneuryisms, and neovascularization (Zongchao et al., 2013; Alistar et al., 2005, Wright et al, 2012). Around 5-10 months, altered astrocyte and microglial morphology along with the apoptosis of retinal cells has been described (Zongchao et al, 2013; Alistar et al., 2005). The average life span of the male

Akita mice however is 305 days or around 10 months while the average life span of the female Akita mice is the same as the C57BL/6J, so many of these retinal changes do not develop until near death for these mice (Yoshioka et al., 1997).

In the DB mice, there is a severe increase of blood glucose and insulin levels 4-6 weeks of age (Coleman, 1978). At even 3-4 weeks of age, the mice are bigger than their WT litter mates. These mice can range from transient to progressive hyperglycemia and these are correlated with pancreatic β cell necrosis and islet atrophy like their type 2 counterparts in humans (Katsuda et al, 2013) At around 5 months the DB mice have decreased creatinine clearance and increased albumin in the urine (albuminuria) (Allen et al., 2004; Sharma et al., 2003). Like the Akita mice, DB mice also have pericyte and endothelial cell loss, increased blood flow, and basement membrane thickening at 6 months of age (Midena et al., 1989; Clements et al., 1998; Tadoyoni et al., 2003). The earliest time point found for formation of acellular capillaries is at 34 months as described by Chou et al., and around 15 months, there is BRB breakdown, and possible neovascularization (Chou et al., 2014; Cheung et al., 2005). However, the average life span of male DB mice is around 349 days or 12 months while the female DB mice life span is around 487 days or 16 months and thus, like the Akita mice, many of the retinal changes do not develop until near death (Sataranatarajan et al., 2016).

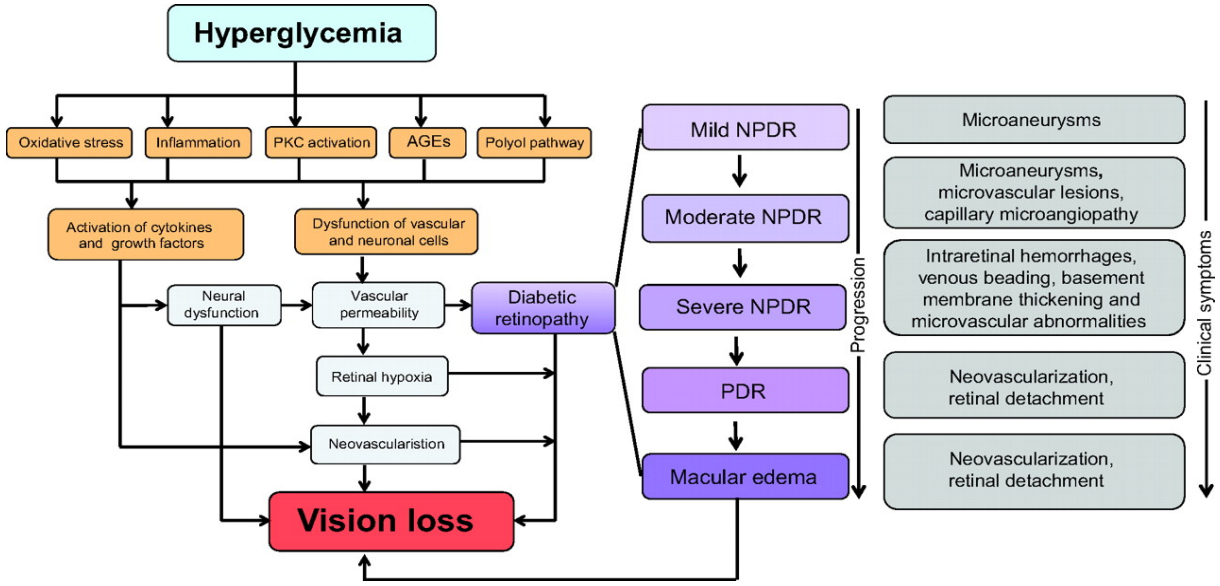


Figure 4. Chart of relation between hyperglycemia and effects upon DR. Hyperglycemia effects upon factors that lead to endothelia cell loss and eventually vision loss. The stages of DR along in relation to the cellular dysfunction. Taken from Robinson et al., 2012.

### 1.5 Hyperglycemia effects upon DR

The exact mechanism whereby increased blood glucose (hyperglycemia) initiates vascular and neuronal alterations is not well understood. Figure 4 shows some proposed mechanisms (Curtis et al., 2009, Villarroel et al., 2009, Robinson et al., 2012). Hyperglycemia can induce many things like; oxidative stress, advanced glycation end products (AGEs), protein kinase C (PKC) activation, increased flux through the polyol pathway, and inflammation, though there has been no human studies examining these yet (Robinson et al, 2012; Frank, 2004; Cheung et al., 2010). These different mechanisms can then eventually lead to pericyte apotosis.

Hyperglycemia causes the activation of the polyol pathway. Polyol initiates the reduction of glucose to sorbitol and then is metabolized to fructose (Oates, 2002). The fructose produced can then be converted to fructose-3-phosphate and 3-deoxyglucosone, both of which are powerful glycosylating agents, which increases the formation of AGEs (Szwergold et al., 1990). The increase of glycosylating agents along with the glucose itself forming covalent bonds with

the protein (glycation) results in AGEs formation. This glycosylation, along with the non-enzymatic glycosylation of proteins often results in disrupted function including the alteration of enzyme activity, decreased receptor recognition, molecular conformation changes, and can lead to a non-functional protein (Hsieh et al., 2007). The increase of fructose and sorbitol along with the formation of AGEs can increase the amount of reactive oxygen species (ROS) (Drummond et al., 2011; Lassègue et al., 2003). Glycation has been shown to decrease platelet derived growth factor homodimer subunit BB (PDGF-BB) activity in-vitro, which may eventually lead to pericyte cell death (Nass et al., 2010; Stitt et al., 2004).

Receptor for advanced glycation end products (RAGE) is present on many cells in the body, including some pericytes, endothelial cells, microglia, and Müller glia cells. AGEs and the increase of ROS are toxic to pericytes and can cause cell death (apoptosis) (Chibber et al., 1997). AGEs can also cause more oxidative stress, inhibition of protein kinase B (AKT) phosphorylation, and reduced platelet derived growth factor ββ (PDGFβ) signaling (Stitt et al., 2004). AGEs can also cause an upregulation of VEGF leading to an increase of neovascularization and angiogenesis (Singh et al., 2014).

These different mechanisms can cause release or alter activation of growth factors like vascular endothelial growth factor (VEGF) and platelet derived growth factor (PDGF), cytokines like interferon gamma (IFN-γ) or interleukin 6 (IL-6) or directly cause dysfunction of cells like pericytes or astrocyte activation. The loss of pericyte is often the first sign of DR. Pericyte loss can then lead to vascular permeability which then can start the DR cascade chain of events.

### 1.6 PDGFRβ Signaling Pathway

One of the important factors altered by hyperglycemia are growth factors, including platelet-derived growth factors (PDGFs).

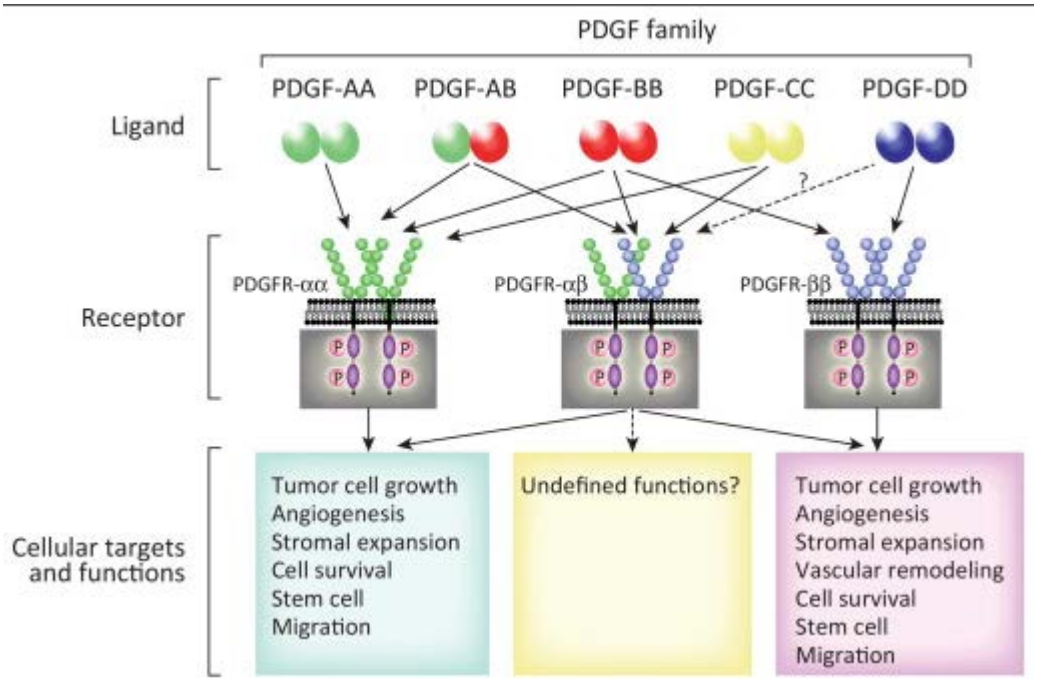


Figure 5 Chart of all PDGF ligands, receptors, and functions of the receptors. PDGF homo and heterodimers along with the homo and hetero receptors and the downstream functions. Taken from Cao, 2013.

As seen from Figure 5, PDGF are a family of polypeptides that can form homo or heterodimers (Cao et al., 2013). The homo or hetero dimers, like PDGF-AA can then bind to the homodimerized receptor, PDGFRββ or PDGFRαα, or heterodimerized receptor PDGFRαβ (Cao et al., 2013). Not all cells contain all receptors. Pericytes express PDGFRβ; however, astrocytes express only PDGFRα. Platelet derived growth factor homodimer subunit BB (PDGF-BB) is important for the not only pericyte viability but important for maintaining the vasculature of the eye. Loss of PDGF-BB in mice often results in vascular abnormalities, increased pericyte loss, capillary dilation, and endothelial cell hyperplasia (Leveen et al., 2004; Lindahl et al., 1994; Hellstrom et al., 1999; Hellstrom et al., 2001, Hammes et al., 2002). Hyperglycemia can induce src homology domain 2 containing inositol-5-phosphatase (SHP-1) resulting in de-

phosphorylation of the receptor and leading to increased pericyte apoptosis (Geraldes et al., 2009). PDGFRβ signaling results in activation of two major pathways the phosphoionositide 3-kinase (PI3K) / protein kinase B (AKT) pathway and the mitogen-activated protein kinase (MAPK)/ extracellular signal-regulated kinases (ERK) pathways that results in the proliferation and survival signaling in pericytes as seen in Figure 6.

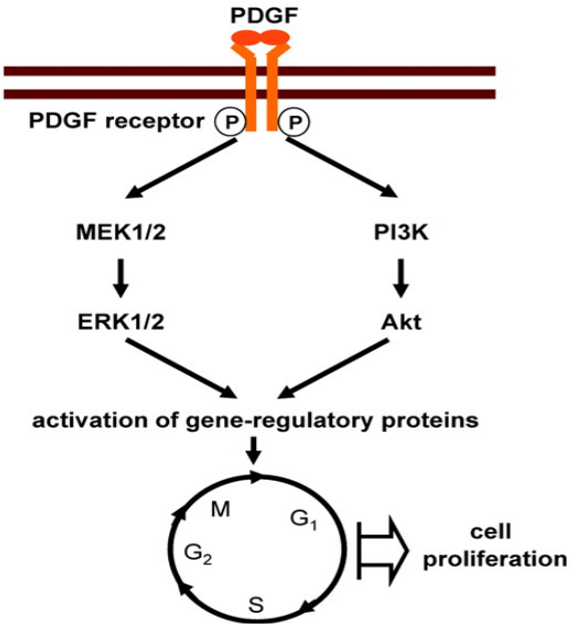


Figure 6 PDGF-BB Downstream activation of ERK and AKT pathways. PDGF-BB phosphorylation leads to activation of ERK and AKT which regulate cell proliferation and survival. Taken from Deuse et al., 2010.

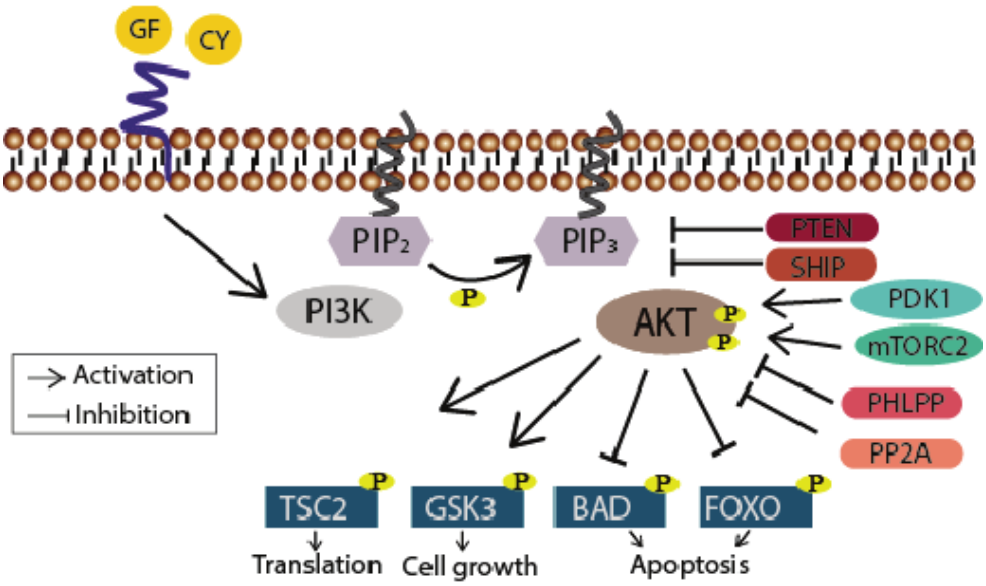


Figure 7. PI3K/AKT signaling pathway. Taken from Diehl and Schall 2013

### 1.7 PI3K/AKT Signaling Pathway

Ligand binding to the PDGFRβ results in the activation of PI3K, leading to phosphorylation of membrane bound phosphatidylinositol (PtdIns), in this case phosphatidylinositol 4,5-bisphosphate ($PIP_2$), converting it into phosphatidylinositol-3,4,5-trisphosphate ($PIP_3$). This can cause cytosolic AKT to dock to $PIP_3$ and opening of the tyrosine phosphorylation site to phosphoinositide-dependent kinase (PDK1) and serine phosphorylation site by mammalian target of rapamycin complex 2 (mTORC2) (Diehl and Schall, 2013). AKT can also be stimulated through a PI3K-independent pathway using DNA-dependent protein kinase (DNA-PK) (Diehl and Schall, 2013). The phosphorylation of AKT then causes it to translocate to the cytosol and nucleus where many of the downstream targets are found (Nicholson and Anderson, 2002).

AKT can upregulate proliferation signaling, and also downregulate apoptotic signaling (Brunet et al., 2001). The downstream target phosphorylation tuberous sclerosis protein 2 (TSC2) which leads to a deactivation of TSC2 and upregulation of mTORC1, which then results

in increased transcription and increased mitochondrial activity (Zarogoulidis et al, 2014). AKT also inactivates glycogen synthase kinase 3 (GSK3), resulting in the prevention of cyclin D1 degradation, and thus causing promotion of the cell to undergo G1 phase progression (Alao, 2007). AKT inhibits Bcl-2-associated death promoter (BAD) and transcription factor Forkhead Box O (FOXO), both which promote apoptosis. AKT can also be deregulated directly or indirectly. Phosphatase and tensin homolog (PTEN) and src homology domain 2 containing inositol-5-phosphatase (SHIP1) both can dephosphorylate $PIP_3$ while protein phosphatase 2A (PP2A) or the H domain and leucine-rich repeat protein phosphatase (PHLPP) can dephosphorylate AKT directly (Diehl and Schall, 2013).

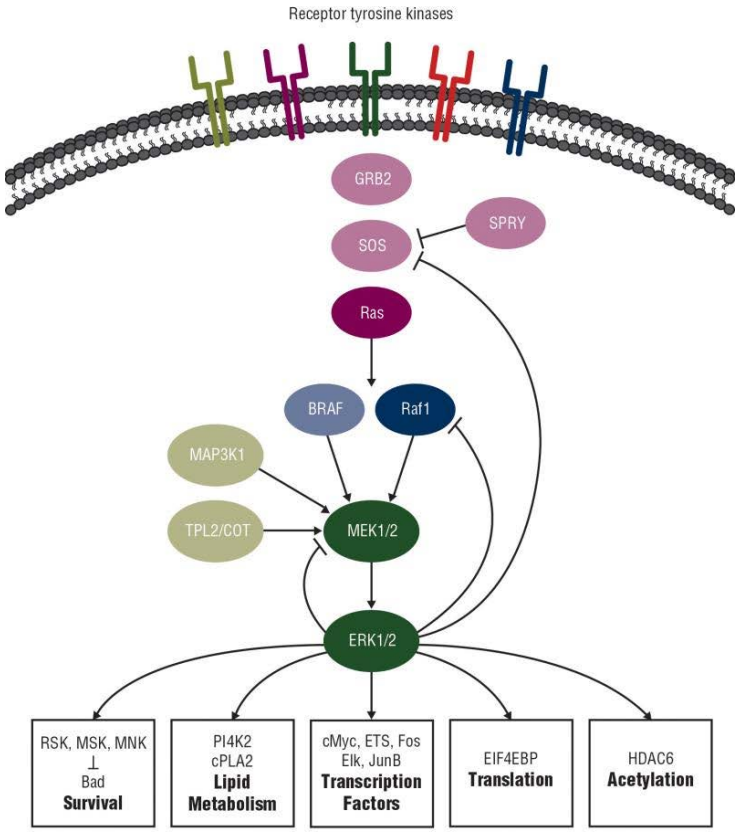


Figure 8 RAS-RAF-MEK-ERK pathway. Taken from Johnson et al., 2014.

### 1.8 ERK Signaling Pathway

The other pathway that PDGFRβ can activate is the MAP kinase kinase kinase (MAP3K) pathways seen in Figure 8. There are multiple different MAPK pathways, each containing a cascade of kinases. For the ERK pathway, the binding of PDGF-BB to the receptors causes phosphorylation by docking proteins such as growth factor receptor-bound protein 2 (GRB2) using the Src Homology 2 (SH2) domain. The docking protein will then use SRC Homology 3 (SH3) to bind to guanine nucleotide exchange factor (GEF) SOS that assists the small GTPAse RAS in exchanging GDP for GTP, a step that activates the RAS. RAS then binds to and activates rapidly accelerated fibromosarcoma (RAF). There a 3 different RAFs, Raf-1 proto-oncogene (RAF1/CRAF), B-Raf proto-oncogene, and Serine/threonine-protein kinase (A-Raf), all of which activate mitogen activated protein kinase kinase (MEK). This MEK can then directly phosphorylate the MAPK or ERK1/2. The two isoforms of ERK, ERK1 or 2 phosphorylate or activate important transcription factors ETS domain-containing protein (Elk-1) and tumor suppressor protein (p53) (Shaul and Seger, 2007).

Ribosomal S6 kinase (RSK), mitogen and stress activated protein kinase (MSK), MAPK interacting serine/threonine-protein kinase (MNK) are other kinases that can inactivate BAD and inhibit apoptosis. ERK1/2 can directly activate transcription factors such as cMYC, ETS, and ELK, translation factors such as EIF-43BP, change chromatin modification such as histone deacetylase 6 (HDAC6), or activate lipid phosphatases such as PI4K2A and phospholipase A2 (PLA2) ( Treisman, 1996; Williams et al., 2013). The ERK pathway can self-regulate by using sprouty (SPRY), an inhibitor of RAS, or directly inhibit RAF, MEK, and RAS through negative feedback loops (Johnson et al., 2014). The ERK pathway is self-contained as RAF1, MEK1/2, and other kinases loops can activate other MAPK pathways such as c-jun N-terminal kinases

(JNK) or Janus kinase (JAK)/ Signal transducer and activator of transcription protein (STAT) pathways or these other pathways can also activate ERK.

### 1.9 Mechanisms of Pericyte Apoptosis

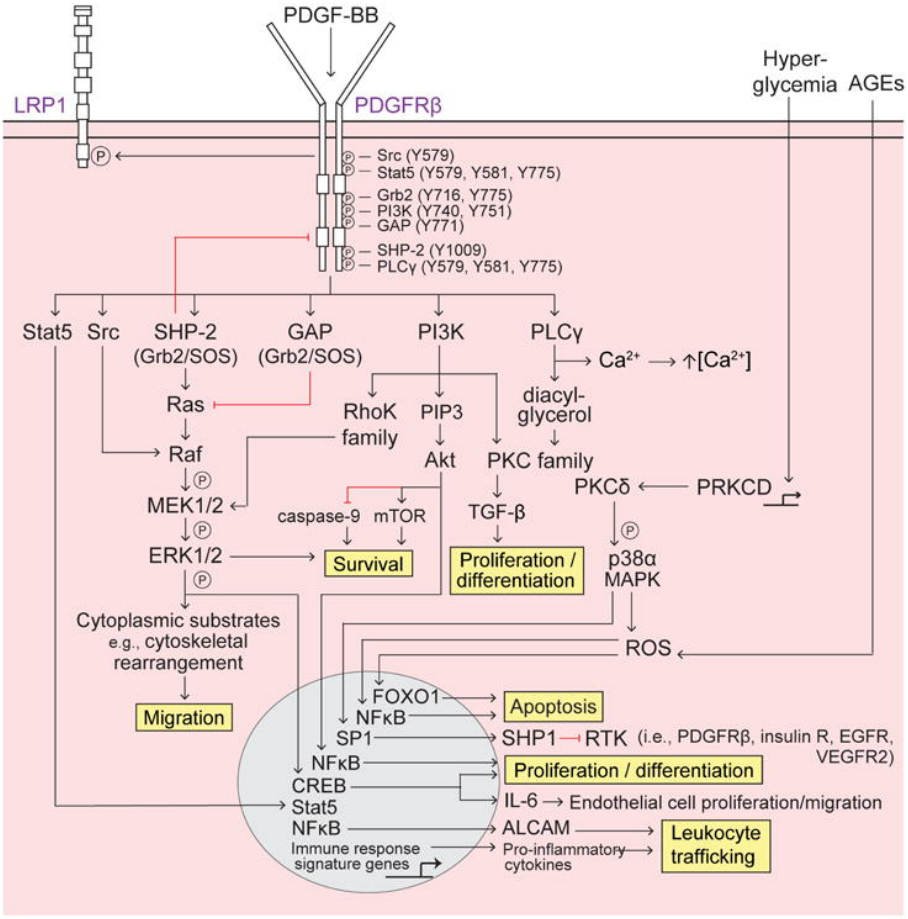


Figure 9 PDGF-BB receptor activation and inactivation. Sweeney et al., 2016.

Figure 9 displays normal PDGF signaling in pericytes and what happens in diabetes. A decrease in PDGFRβ signaling leads to pericyte apoptosis (Sweeney et al., 2016). AGEs from hyperglycemia can directly increase ROS which can then activate the FOXO pathway and lead to apoptosis. AGEs can also decrease AKT signaling through the increase of SHP1 and also decrease PDGFRβ signaling overall. Increases in SHP1, a phosphatase, leads to not only increases in the dephosphorylation of both ERK/AKT pathways but also inactivation the

PDGFR-ββ phosphorylation itself (Geraldes et al., 2009). There is also increased ROS from other sources that can lead to apoptosis through the nuclear factor kappa-light-chain-enhancer of activated B cells (NFκB) activation (Romeo et al., 2002). NFκB, a transcription factor, when activated can induce production of cell survival and proliferation (Ben-Neriah and Karen, 2011). Although NFκB can lead to proliferation, in type 2 diabetics with nonproliferative retinopathy NFkB leads to pericyte apoptosis (Romeo et al., 2002).

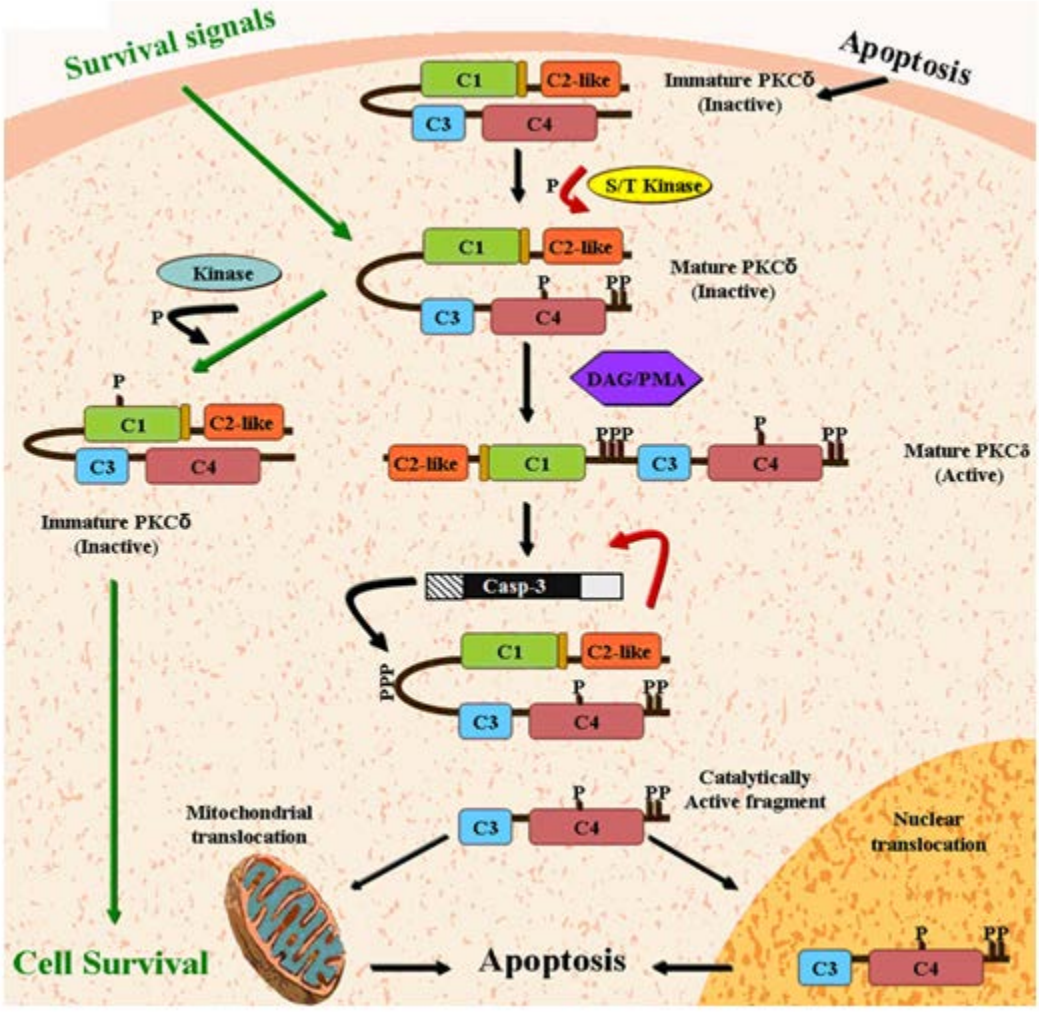


Figure 10 PKCδ inactivation and activation by caspase 3. Taken from Malvez et al., 2009.

### 1.10 PKCδ Signaling Pathway

Another mechanism of apoptosis is through the PKCδ activation as shown in Figures 9 and 10. PKCδ and other isoforms are normally inactive in the cell and require activation by diacylglycerol (DAG). After phosphorylation at the threonine and serine sites, PKCδ undergoes a conformational change exposing the regulatory unit and catalytic unit (Steinberg, 2004). This change can allow caspase 3 to cleave the PKCδ and separate it into two units, a regulatory and catalytic unit (Malvez et al., 2009). The catalytic unit translocates into the nucleus where it can activate transcription factors regarding apoptosis (Malvez et al., 2009). This unit can also be activated without translocation to the membrane (Steinberg, 2004). Caspase 3 not only cleaves PKCδ, but caspase 3 is also a substrate of active PKCδ, thus this system can operate in a feedback loop to regulate apoptosis (Basu, 2003). The translocation of PKCδ into the nucleus can cause the inactivation of proteins, like nuclear DNA-dependent protein kinase (DNA-PK) (Brodie and Blumberg, 2003). The inactivation of DNA-PK through PKCδ can result in the inhibition of DNA repair and enhanced DNA fragmentation (Brodie and Blumberg, 2003).

### 1.11 Reactive Gliosis

Reactive gliosis, the activation of macroglia, astrocytes and Müller glia, and microglia, can also play a role in inflammation and DR. Reactive gliosis can often include proliferation, extracellular matrix (ECM) remodeling, hypertrophy, and expression patterns. At first, this change is positive as it induces activation of proliferation signaling (Burda et al., 2014). However, chronic gliosis can result in scar formation, remodeling of the vasculature, and neuronal cell death (Burda et al., 2014). Gliosis can have a wide range of changes involving different proteins. For Müller glia and retinal astrocytes, glial fibrillary acidic protein (GFAP), toll like receptor 4 (TLR-4), vimentin (VIM), epidermal growth factor receptor (EGFR),

glutamine synthetase (GS), matrix metalloproteinase (MMP), tissue inhibitor of metalloproteinase (TIMP), neurocan core protein (NCAN), phosphacan (PCAN), glutamate aspartate transporter (GLAST), and many others (Dharmarajan, et al., 2017; Zamanian et al., 2012).

Intermediate filaments, like GFAP and VIM, help support the structure of cells and provide mechanical support for the cell membrane (Lodish et al., 2000). Other proteins are involved in extracellular matrix homeostasis including; NCAN, PCAN, MMPs, and TIMPs (Frantz et al., 2010). Growth factors, like EGF and colony stimulating factors (CSF), help maintain cell growth and function. GLAST and GS mediate neurotransmitter, specifically glutamine, release and reuptake (Derouiche and Rauen, 1995). Pattern recognition receptors (PRRs), like TLR-4, are important for mediating innate and humoral immunity in the body and retina (Lee and Kim, 2007).

Astrocytes play a big role in reactive gliosis, as they are the main glial cell that undergoes changes when reactive gliosis happens in DR. In astrocytes, GFAP, VIM, GS, and S100 calcium-binding protein-β (S100β) are the major markers that get upregulated in the event of reactive gliosis (Rideta et al., 1997). Other markers like ECM chondroitin sulfate proteoglycans (NCAN/PCAN), MMP, TIMP2, GLAST, and have also been found to be increased in reactive gliosis in astrocytes (Sofronview, 2009). The proteoglycan production (NCAN/PCAN) in astrocytes following reactive gliosis inhibits axonal outgrowth and regeneration (Silver and Miller, 2004). MMPs also exhibit increased expression by astrocytes, resulting in glial scar formation through breakdown and remodeling of the ECM along with attraction of astrocytes to the injured area (Hsu et al., 2008). TIMP2, a regulator of MMPs, is highly expressed in reactive astrocytes suggest that they help with MMP regulation while also possibly separating damaged

retinal areas from undamaged areas (Agapova et al., 2003). The GFAP and VIM are important intermediate filament proteins for astrocytes and the upregulation of GFAP and VIM in astrocytes can cause hypertrophy, activate the astrocyte and can slow down the regeneration of the injured area (Pekney and Nilsson, 2005). GLAST and GS maintain glutamine regulation and an increase of GLAST and Gs can lead to decreased glutamate excitotocity (Maragakis and Rothstein, 2006). There is an increase in growth factor release (EGF) and increased expression of growth factor receptors (EGFR), thus causing increased proliferation and survival signaling (Sardar et al., 2017). Many inflammatory cytokines and chemokines are also released during reactive gliosis by the astrocytes (Sofroniew, 2009).

Müller glia, like astrocytes, undergo proliferation, change ion transport properties, change in intermediate filament production, and can secrete molecules like VEGF through many of the same mechanisms (Dyer and Cepko, 2000). GFAP and VIM upregulation in Müller glial cells causing cell shape alterations is one of the hallmarks of reactive gliosis, as there is little GFAP and VIM before reactive gliosis (Lewis and Fisher, 2003). Müller glia also, like astrocytes, can undergo proliferation, change ion transport properties, and can secrete molecules like VEGF (Dyer and Cepko, 2000). This is mostly likely induced by either the loss breakdown of the BRB or hyperglycemia induced apoptosis (Bringmann et al., 2006). The growth factor release of VEGF, along with other angiogenic cytokines, can cause the increase of MMP's by endothelial cells (Bringmann et al., 2006). Changes in Möller glia can also not only increase inflammatory cytokine release, but it can also increase the production of nitric oxide (Bringmann et al., 2006). Möller glia cells can have decreased ion and water transport resulting in serum leakage and increased glutamate in the environment (Bringmann et al., 2006).

Changes in Müller glia and astrocytes during reactive gliosis can also cause changes in microglia (Dharmarajan et al., 2017). Besides cell number, morphology, movement, and surface molecular changes, microglia can release cytotoxic substances, ROS, excitatory amino acids, and an increase in proteases, thus causing neuronal death (Kreutzberg, 1996). The microglia have been shown to precede many macroglia changes and upon activation macroglia can then feedback to the microglia (Zeng et al., 2008). Microglia changes can be seen 4 weeks before even the first change in GFAP in Müller cells (Barber et al., 2005).

In early reactive gliosis, microglia act in a protective manner to help clean up debris and secrete wound healing factors (Kreutzberg, 1996). However, in prolonged gliosis, microglia can bring about neuronal demise and other important cells (Streit et al., 1999). The activation of microglia in DR can be seen to be caused by AGE, inflammatory signals, growth factors such as bone morphogenetic protein, generation of oxidative stress, or even by hyperglycemia itself (Grisby et al., 2014, Dharmarajan, et al., 2017).

### 1.12 Inflammation

Hyperglycemia, glycation, oxidative stress, AGE, reactive gliosis, and pericyte death can lead to an increase in inflammation in the retina, which may trigger gliosis **(**Tang and Kern, 2011**).** Inflammation is the body's non-specific immune response to injury and often results in elevated metabolism, vasodilation, increased blood flow, release of cytokines and chemokines, cellular influx, and extravasation of fluids and cellular influx (Ferror-Milani et al., 2007). It is normally an acute response and self-limiting, but in some cases these processes can become continuous and thus become known as chronic inflammation (Ferror-Milani et al., 2007). Changes in chemokine and cytokine release as seen in Figure 11 can often be the differentiation factors between acute and chronic inflammation. The interleukins (IL) have a split role with IL-

8, IL-16 along with granulocyte-colony stimulating factor (G-CSF) mainly playing a major role in acute inflammation while IL-1, 6, 11, 17 play an important role in both. IL-2 through 5, IL-7, IL-9, IL-10, IL-12 through 15 along with interferons (IFN) gamma and alpha, tumor necrosis factors (TNF) alpha and beta, transforming growth factor (TGF) beta, and granulocyte macrophage stimulating factor (GM-CSF) all play an important role in chronic inflammation. There are some factors that affect both acute and chronic inflammation and may serve as mediators of acute versus chronic, like IL-1 (Feghali and Wright, 1997). There are other factors that affect inflammation like interferon regulatory factor 8 (IRF8), cluster of differentiation 68 (CD68), allograft inflammatory factor 1 (AIF-1/IBA-1), thrombospondin (THBS), and chemokine ligand 5 (CCL5) or better known as regulated on activation, normal T cell expressed and secreted (RANTES).

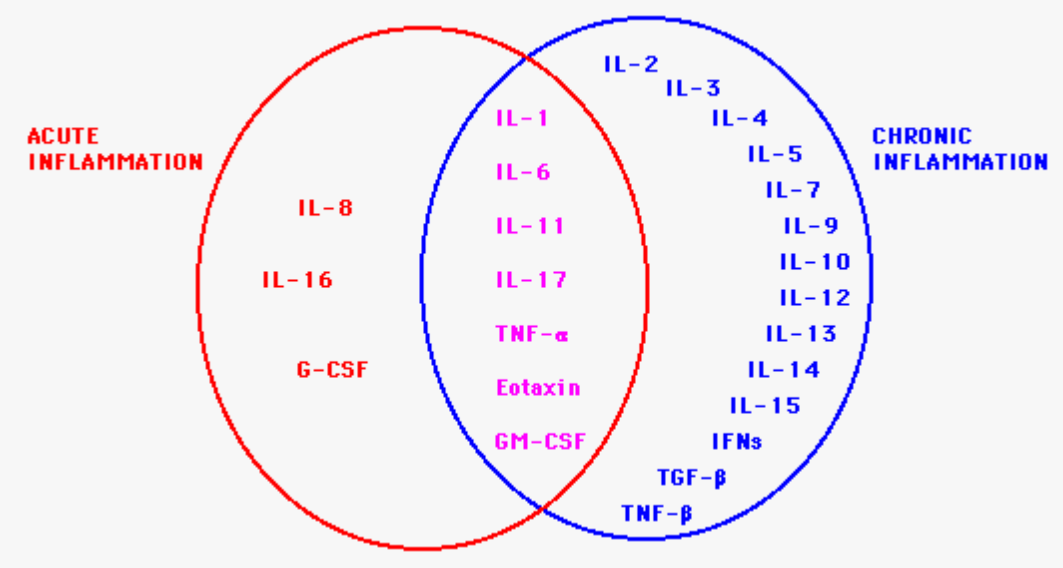


Figure 11 Cytokines involved in acute versus chronic inflammation. Taken from Feghali and Wright (1997).

IL-1, IL-6, TNF-α, and maybe IL-8 are thought to be the more major initiators and mediators of acute inflammation, though they can be active in chronic inflammation as well (Gabay and Kushner, 1999). IL-1 and its two isoforms, alpha and beta, trigger fever, increase

prostaglandin synthesis, activate T-cells, activate B cells and antibody production, initiate neutrophil activation and influx, and cause fibroblast proliferation (Keyel, 2014). IL-6 is thought to be the main stimulator of many of the acute phase proteins (Gabay and Kushner, 1999). IL-6 is more thought to be a systemic activator of inflammation (Gabay, 2006). IL-6 can be anti-inflammatory in early acute inflammation, and can cause reduction in the pro-inflammatory markers, like IL-1β and TNF-α (Tilg et al., 1994). Later during the inflammatory process, IL-6 is thought to be pro-inflammatory (Scheller et al., 2011). IL-6 can activate and recruit neutrophils, but IL-6 also can recruit monocytes, like macrophages (Gabay, 2006). IL-6 induces humoral responses, like T-cell activation and B-cell differentiation (Gabay, 1999). TNFα, like IL-6, is an important homeostatic regulator of pathogen defense, apoptosis, tissue regeneration, and necrosis (Kalliolias and Ivashkiv, 2015). TNFα can recruit inflammatory cells (causing release of growth factors, adhesion molecules), induce necroptosis, induce other inflammatory cytokine release, and cause proliferation of immune cells (Kalliolias and Ivashkiv, 2015).

Interferons, pro-inflammatory cytokines, are another major family that mediates inflammation. There are two major groups of interferons, type 1 (IFNα and IFNβ) and type 2 (IFN-γ). Type 1 interferons are thought to be involved in maintaining T-cell regulation and regulating apoptosis (Akbar et al., 2000). IFNα helps prolong T-cell activation and prevents apoptosis of T-cells, thus possibly providing memory in T and B cells (Akbar et al., 2000). IFN-γ has been shown to enhance major histocompatibility complex (MHC) class I and II expression while also priming and activating macrophages for phagocytosis (Feuerer et al., 2006). MHC's are important for the regulation of the innate and humoral immunity, specifically the response of the different T cells (Swain, 1983). IFN-γ has been shown to transition the immune response to helper type 1 (Th1) rather than helper type 2 (Th2) while affecting TNFα response (Farrar and

Schreiber, 1993). Th1 signals innate immune system responses recruiting and activating macrophage and cytotoxic T cells while producing a pro-inflammatory environment by releasing factors like IFN-γ and TGF-β (Singh et al., 1999). Th2 signals the adaptive immune system recruiting $CD4^+$ T cells and B cells and producing an anti-inflammatory response by releasing factors like IL-10 and IL-4 (Singh et al., 1999).

Different growth factors, like VEGF, GM-CSF, and G-CSF, have a role in the immune response of inflammation. The CSF family are involved in the activation and generation of leukocytes from the bone marrow (like macrophages and granulocytes) (Becher et al., 2016). After T and often B cell infiltration caused by IL-6 or IFN-γ, GM-CSF is often released and stimulates the production of monocytes (macrophages and dendritic cells) and granulocytes (neutrophils, eosinophils, and basophils) (Becher et al., 2016). G-CSF; however, produces and activates only granulocytes, primarily neutrophils (Campbell et al., 2016). VEGF is involved in the formation and maintenance of blood vessels (angiogenesis) and the release of VEGF increases leukocyte penetration through increased vascular permeability (Zimmermann and Issekutz, 2006). TGF-β plays a different role in inflammation and the immune response. TGF-β maintains self-tolerance of immune cells while initiating and regulating lymphocytes, natural killer (NK), and macrophages (Ming, 2006).

Along with growth factors, there are a variety of other factors that get either upregulated or downregulated in inflammation. CCL5, chemotaxis marker, is released by macrophages to recruit T cells to the injured area (Marques et al., 2013). THBS is a regulatory marker, not only activating TGF-β but also mediating IL-10, an anti-inflammatory agent (Lopez-Dee et al., 2011). Interferon regulatory factor (IRF) is regulator marker that regulates the activation or repression of the IFN's (Taniguchi et al., 2001). IRF8 is induced by IFN-γ and important for myeloid cell

and lymphoid cell differentiation (Taniguchi et al., 2001). CD68 and IBA1 are markers for activated microglia and macrophages during the inflammatory process (Chiu et al., 2009).

Diseases, like diabetes and arthritis, often result in a chronic inflammatory state. Pro-inflammatory factors, such as IL-6 and TNF-α, often are elevated in diabetic patient when compared to their non-diabetic counterparts and correlate with insulin resistance (Navarro and Mora, 2006). Obesity, associated with type 2 diabetes, impacts inflammation as adipocytes may cause the release of IL-6, C reactive protein (CRP), and TNFα (Dandona et al., 2004). Inflammation can be attributed to continuous pancreatic β cell death in type 1 diabetics (Eizirik et al., 2009). The activation of pattern recognition receptors (PRR), like TLR-4, activates the innate immune response and increases in IFN, IL-1, and TNF (Eizirik et al., 2009). These different chemokines and cytokines attracts macrophages and neutrophils which then release factors like Chemokine (C-C Motif) Ligand 2 (CCL2). The increase of ER stress from activation of TLR may cause β cell apoptosis, which along with macrophages activation, can eventually lead to the activation of the adaptive immune system (Eizirik et al., 2009). This loop continues and eventually leads to suppression of β cell function and proliferation, thus leading to β cell death (Eizirik et al., 2009).

Apoptosis is only one of the causes of inflammation (Tang and Kern, 2011). Hyperglycemia produces a pro-inflammatory environment (Tang et al., 2011). Increases in fatty-acid composition can cause chronic inflammation in the retina (Byeon et al., 2010). Oxidative stress causes increases Il-1β and NF-κB (Kowluru and Odenbach, 2004). AGE/RAGE increase the proinflammatory environment while also decreasing anti-inflammatory effects (Li et al., 2011).

Inflammation changes affect the retina and eye differently than in other parts of the body. CCL-2, IL-1β, TNF-α, and VEGF are just some of the inflammatory factors that have been found to be increased in DR (Tang and Kern, 2011). Increases in VEGF production results in increases in vascular permeability and genesis of new capillaries, leading to breakdown of BRB (Tang and Kern, 2011). Leukocyte migration to the BRB may trigger endothelial cell apoptosis (Joussen et al., 2003). Microglia become activated in high glucose states and the microglial activation releases proinflammatory and cytotoxic factors (Tang et al., 2011). Müller glia, through activated RAGE signaling, leads to VEGF and other cytokines release (Du et al., 2004). Pericytes, in hyperglycemia conditions, releases factors like IL-1β, NF-κB, VEGF, TNF-α, and TGF-β, and these factors stay increased even when there is a loss of high glucose environment (Kowluru et al., 2010).

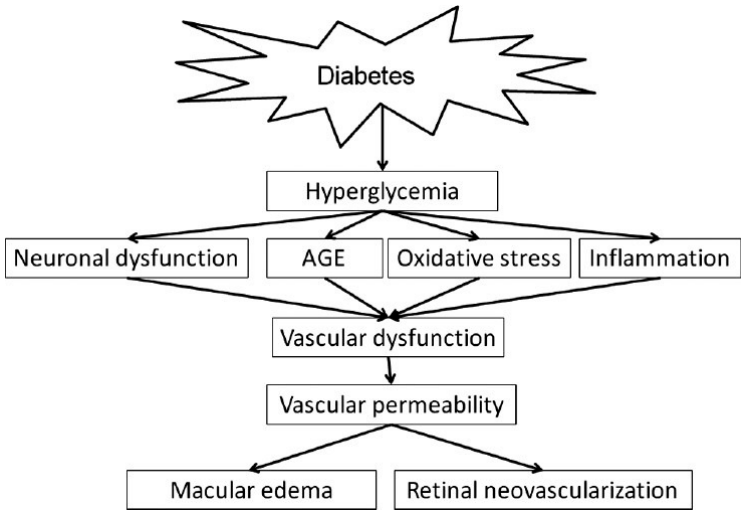


Figure 12 Hypothesis on how diabetes and hyperglycemia causes DR. Taken from Shin et al., 2014.

### 1.13 Focus for study

The inflammatory changes, along with AGE/RAGE and ROS, can often lead to the progressive nature of DR as seen from Figure 12. However, the relationship between pericyte

loss and inflammation is not well established (Tang and Kern, 2011). The cause of pericyte loss could be due to inflammation, AGE/RAGE, and/or oxidative stress. All these changes will affect PDGFRβ signaling and the downstream pathways. These changes are hard to see in humans, as most people who get early symptoms of DR often already the moderate to late stage DR. However, even with animal models, most studies are done with animals presenting after hyperglycemia and pericyte loss are complete. This study addresses when various pro-inflammatory molecules are present in relation to pericyte loss, gliosis, and vascular changes and directly tests a role for γ-γ in pericyte health.

# 2. MATERIALS AND METHODS

## 2.1 Isolation and Culture of Pericytes

Pericyte cells were cultured in DMEM Sigma medium containing [a mixture of DMEM (D5523 Sigma), penicillin/streptomycin, glutamax, 10% FBS and 44 U/ml of interferon-γ (IFN-γ; R&D systems)]. In acute treatments, pericytes were grown to confluence with 5%CO2 at 33 °C and passaged every 2-3 days using trypsin-EDTA. After the plating on 6 well-plates, cells were treated with ranging from 1-100 ng/ml mouse interferon-gamma (IFN-γ; R&D systems), 1 μl/ml vehicle (4 mM HCL), 1μl/ml of PBS, or 40-80ng/ml of PDGF-BB (recombinant human PDGF-BB; R&D systems). After 24 hours of incubation, pericytes were either treated with IFN-γ or PBS for 24 hours. Then PDGF-BB or 4mM HCL was added for 30 minutes before harvesting for RNA isolation and protein extraction. In chronic treatments, pericytes were plated and incubated between 24-48 hours. After incubation, media was removed and washed with DMEM + 10%FBS before the addition of media containing IFN-γ or PBS. Pericytes were treated with IFN-γ for 24 hours for 3 days. After 72 hours of treatment, 50 ng of PDGF-BB or vehicle (4mM HCL) was added and incubated for 30 minutes before harvesting and for protein extraction, RNA isolation, or immunocytochemistry.

## 2.2 Western Blotting

Cells were washed and before being scraped and centrifuged for 10 mins at $4^0$C at 12,000 RPM. After incubation on ice in lysis buffer (150 mM NaCl, 50mMTris pH 8.0, 2 mM EDTA, 5% TritonX-100; 100 mM PMSF, protease inhibitor cocktail (p50700-1, RPI corp) and phosphatase inhibitor cocktail (P0044, Sigma) for 15 mins protein was then for 10 mins at $4^0$C at

12,000 RPM. Total protein concentration was then was determined using BCA protein Assay reagent (Thermo Scientific). Five µl of sample was mixed with 500 µl of working reagent (prepared by mixing Pierce BCA Reagent A and B in 50: 1 ratio) and 495 µl of water. This solution was incubated at 65 °C for 30 min, followed by colorimetric analysis using a NanoDrop 2000c spectrophotometer (Thermo Scientific). 50 µg of total protein mixed with the loading dye at a 3:1 ratio was then loaded and run on a 4%–20% SDS polyacrylamide gel (Expedeon, San Diego, CA) at 125 V for 1 h. Proteins were transferred to a polyvinylidene fluoride (PVDF) membrane (Bio-Rad) via a wet transfer at $4^0$C for 90 mins at 100V and subjected to immunoblotting. Prior to immunoblotting, some membranes was subject to Western Blot Enhancer Signal treatment kit (Thermo Scientific 46641). This involved washing the membrane 3X with ultrapure water then incubation with Antigen Pretreatment Solution for 10 mins at room temperature (RT) before washing 5X with ultrapure water. The membrance was then blocked with either 5% milk in tris buffered saline tween 20 (TBST) or 10% BSA in TBST (TBST; composition – 20 mM Tris base, 137 mM sodium chloride, 1 M HCl, 0.1% Tween-20, at pH 7.6) at RT for 1 h on a shaker. The blots were incubated with primary antibody-diluted TBST at 4 °C overnight on a shaker. The following day, the blots were washed 3X at 10 minutes and 1X at 5 minutes with TBST and incubated with HRP conjugated secondary in TBST for 1 hr at RT. Blots were washed 3X for 10 minutes and 1X for 5 minutes in TBST, incubated with super signal west femto or super signal west pico plus chemiluminescent substrate (Thermo Scientific), and visualized on x-ray films.

Table 1 List of Western Blot Antibodies

| Antibody | WB concentration | Catalog # | Vendor | RRID # |
|---|---|---|---|---|
| Phospho-PDGFRB | 1:1000 | MAB9027 | R&D Systems | AB_2162777 |
| PDGFRB | 1:1000 | 3169 | CST | AB_2162497 |
| Phospho-p44/42 MAPK | 1:1000 | 9101 | CST | AB_331646 |
| P44/42 MAPK | 1:1000 | 9102 | CST | AB_330744 |
| Phospho-Akt | 1:1000 | 4060 | CST | AB_2315049 |
| Akt | 1:1000 | 2920 | CST | AB_1147620 |
| PKC-δ Antibody | 1:1000 | Gtx50605 | Gene Tex | AB_11162869 |
| B-tubulin | 1:1000 | T0198 | Sigma | AB_477556 |
| Peroxidase-Conjugated Goat anti-Rabbit | 1:4000 | 32460 | Thermo Scientific | AB_1185567 |
| Peroxidase-Conjugated Goat anti-Mouse | 1:4000 | 32430 | Thermo Scientific | AB_1185566 |
| Goat anti-Rabbit IgG, HRP- linked antibody | 1:8000 | 7074 | CST | AB_20999233 |
| Horse anti-Mouse IgG HRP-Linked antibody | 1:8000 | 7076 | CST | AB_330924 |

### 2.3 Flat Mount Immunohistochemistry

Preparation of retinal flatmounts and immunolabeling was done as described in (Dharmarajan et al., 2017). Briefly, enucleated eyes were washed in 1× PBS, fixed in 4% PFA, transferred to 2× PBS on ice, and followed by retina isolation, four to five radial incisions were made to create a petal shape (Dharmarajan S. et al., 2017). Retinas were transferred to cold methanol (−20 °C). The tissue was washed with 1× PBS before and blocked in Perm/Block solution (1× PBS, 0.3% TritonX-100, 0.2% bovine serum albumin, and 5% donkey or goat serum) for 1hr at RT. The tissue was then washed in PBSTX (0.3% TritonX-100 diluted in 1X PBS) and incubated with primary antibody made in Perm/Block solution (Table 2) overnight at 4 °C. On the following day, the tissue was washed with 2X for 10 minutes each time with PBSTX,

incubated with secondary antibody for 3 hours, washed with 3X for 15 minutes each time with PBSTX, incubated with Hoechst solution, and mounted onto a slide with Aqua Polymount (Polysciences, Inc).

Table 2 List of Immunohistochemistry Antibodies

| Antibody | Flatmount Concentration | Catalog # | Vendor | RRID# |
|---|---|---|---|---|
| GFAP | 1:150 | Z0334 | Dako | AB_10013382 |
| Sox2 | 1:150 | SC17320 | Santa Cruz | AB_22686684 |
| IBA1 | 1:150 | 019-19741 | Wako | AB_839504 |
| NG2 | 1:200 | 05-710 | Millipore | AB_309925 |
| IB4 | 1:300 | I21411 | Thermo Scientific | AB_2314662 |
| Cleaved Caspase 3 | 1:100 | AF835 | R & D Systems | AB_2243952 |
| PCNA | 1:200 | 2586 | Cell Signaling | AB_2160343 |
| Alexa Flour | 1:500 | A-11034, A-11055 | Thermo Scientific | AB_2576217, AB_142672 |

### 2.4 Immunocytochemistry

Methods were followed as decribed Dharmarajan et al., 2017. Briefly, the cells were washed with 1X PBS and then fixed for 1hr in 4% paraformaldehyde (PFA). After washing with 1X PBS, cells were permeabilized in methanol, incubated with 1% SDS in 0.01M PBS, and washed in 1X PBS. The cell were then incubated in 5% serum with 0.25% TritonX-100 in 1X PBS for 1 hour at room temperature. Following removal of blocking solution, cells were incubated at 4°C overnight in 2% serum in 0.025% Triton-X in 1XPBS with the appropriate primary antibody. Following overnight incubation with the primary antibodies, the cells were washed with 1X PBS and incubated 1hr at RT with appropriate

secondary antibody. The slides were then washed with 1X PBS, counterstained with Hoechst solution, and mounted with Aqua polymount.

### 2.5 Reverse Transcriptase-quantitative Polymerase Chain Reaction

Reverse Transcriptase-quantitave Polymerase Chain Reaction (RT-qPCR) was done following the procedure done by Dharmarajan et al., 2014, 2017**.** Using a SYBR green mix (Roche), the reactions were carried out using the LightCylcer480 system (Roche). The change in RNA levels was measured using the $2^{-\Delta\Delta Ct}$ method, where Ct is the crossing threshold/crossing point (Cp) value (Dharmarajan et al., 2017**)**. Relative RNA levels were compared to the control animal and normalized using the geometric means from the Ct value derived from three housekeeping genes: β- 2 Microglobulin (B2M), succinate dehydrogenase complex subunit A (SDHA), and signal recognition particle 14 kDa (SRP14).

Table 3 List of Gliosis Markers

| Gene | Primer | Sequence | Product length |
|---|---|---|---|
| Gfap2 | Forward | TAGCCCTGGACATCGAGATCGCC | 141 |
| | Reverse | GGTGGCCTTCTGACACGGATTTGG | |
| Vim | Forward | AGGAAGCCGAAAGCACCCTGC | 78 |
| | Reverse | TCCGTTCAAGGTCAAGACGTGCC | |
| Gs | Forward | GCGCTGCAAGACCCGTACCC | 145 |
| | Reverse | GGGGTCTCGAAACATGGCAACAGG | |
| Egfr-1 | Forward | ACCTATGCCACGCCAACTGTACCT | 82 |
| | Reverse | TGAACGTACCCAGATGGCCACACTT | |
| Tlr-4 | Forward | TGCCTGACACCAGGAAGCTTGA | 102 |
| | Reverse | AGGAATGTCATCAGGGACTTTGCTG | |
| Pcan | Forward | ATCCCTGAGTGGGGAAGGCACA | 96 |
| | Reverse | AGCAGGGGATGCTGGGTGATGA | |
| Ncan | Forward | CCTGACAAGCGTCCATTCGCCA | 90 |
| | Reverse | ACTGTCCGGTCATTCAGGCCGAT | |
| Timp2 | Forward | GCAACAGGCGTTTTGCAATG | 71 |
| | Reverse | CGGAATCCACCTCCTTCTCG | |
| Mmp14 | Forward | TGGGCCCAAGGCAGCAACTT | 89 |
| | Reverse | CGTTGTGTGTGGGTACGCAGGT | |

Table 4 List of Inflammatory Markers

| Gene | Primer | Sequence | Product length |
|---|---|---|---|
| Gm-Csf | Forward | AGTCGTCTCTAACGAGTTCTCC | 178 |
| | Reverse | AACTTGTGTTTCACAGTCCGTT | |
| Csf1 | Forward | ACCAAGAACTGCAACAACAGC | 91 |
| | Reverse | GGGTGGCTTTAGGGTACAGG | |
| Inf-α | Forward | CAAGCCATCCCTGTCCTGAG | 131 |
| | Reverse | TCATTGAGCTGCTGGTGGAG | |
| Inf-γ | Forward | CAACAGCAAGGCGAAAAAGGA | 90 |
| | Reverse | AGCTCATTGAATGCTTGGCG | |
| Il-1β | Forward | TGTCTGAAGCAGCTATGGCAA | 141 |
| | Reverse | GACAGCCCAGGTCAAAGGTT | |
| Il6 | Forward | ACTTCACAAGTCGGAGGCTT | 111 |
| | Reverse | TGCAAGTGCATCATCGTTGT | |
| VEGF | Forward | ACTGGACCCTGGCTTTACTG | 74 |
| | Reverse | CTCTCCTTCTGTCGTGGGTG | |
| CCl5 | Forward | TGCCCACGTCAAGGAGTATTT | 111 |
| | Reverse | ACCCACTTCTTCTCTGGGTTG | |
| Thbs1 | Forward | GCCACAGTTCCTGATGGTGA | 149 |
| | Reverse | TTGAGGCTGTCACAGGAACG | |
| Thbs2 | Forward | GGGAGGACTCAGACCTGGAT | 105 |
| | Reverse | CGGAATTTGGCAGTTTGGGG | |
| Cd68 | Forward | AAGGGGGCTCTTGGGAACTA | 139 |
| | Reverse | AAGCCCTCTTTAAGCCCCAC | |
| Iba1 | Forward | ACGAACCCTCTGATGTGGTC | 118 |
| | Reverse | TGAGGAGGACTGGCTGACTT | |
| Irf8 | Forward | CGGATATGCCGCCTATGACA | 73 |
| | Reverse | CTTGCCCCCGTAGTAGAAGC | |
| B2M | Forward | AGATGAGTATGCCTGCCGTG | 120 |
| | Reverse | TCATCCAATCCAAATGCGGC | |
| Sdha | Forward | GGACAGGCCACTCACTCTTAC | 130 |
| | Reverse | CACAGTGCAATGACACCACG | |
| Srp14 | Forward | CCTCGAGCCCGCAGAAAA | 134 |
| | Reverse | CGTCCATGTTGGCTCTCAGT | |

### 2.6 Statistics

Flatmounts of all cell counts were imaged using Olympus Fluoview FV 1000 with N=4 or 5. Area was subdivided into two regions up to 1500um$^2$ from the optic nerve, or 2) the area from 1500-300um$^2$ and 3-5 pictures were taken of each area. Quantification was done using NIH image J (Scheinder et al., 2012) and was graphed using scatter dot function of GraphPad Prism. For IB4 vascular staining, the percentage area and branches were determined using AngioTool software (Zudaire et al., 2012). The RT-qPCR results were calculated using the method described by Pfaffl (Pfaffl, 2010) and the values were normalized to a geometric mean of 3 housekeeping genes (N=3). $Log_2$ expression levels were calculated and graphed using Microsoft Excel. In western blots (N=3), densitometry was done using ImageJ and the results were graphed using Microsoft Excel (Scheinder et al., 2012). Immunocytochemistry results were collected and graphed using the scatter dot plot function of GraphPad Prism with the average and error bars shown in black. All statistical significance was determined using a one-way analysis of variance (ANOVA) with a Tukey's multiple comparison test with probability levels of 0.05, 0.001, and 0.001.

# 3. RESULTS

## 3.1 Pericyte loss was evident as early as 3 weeks in the Akita and DB model systems.

The progression of retinal pericyte loss in the Akita and DB models has not been described. Further, there have been few comparative analyses using models of type 1 and type 2 diabetes. To investigate the loss of pericytes in a model of type 1 and type 2 diabetes, retinal flatmounts were immunolabeled for pericyte marker neural/glial antigen 2 (NG2) at 3, 6, 12, 18, and 24 weeks of age in both the Akita and DB models (Figure 13A). A comparative analysis of NG2+ cells indicates there were fewer cells in the Akita and DB retinas in comparison to the wild type (WT) as early as 3 weeks of age (Figure 13B). Both the Akita and DB models lost pericytes at 12 weeks of age (Fig 13B). The number of pericytes in the DB retinas leveled out at the 18 and 24 week time points; however, the number of pericytes in the Akita retina appeared to rebound at 18 weeks and then returned to a lower level at 24 weeks (Figure 13B).

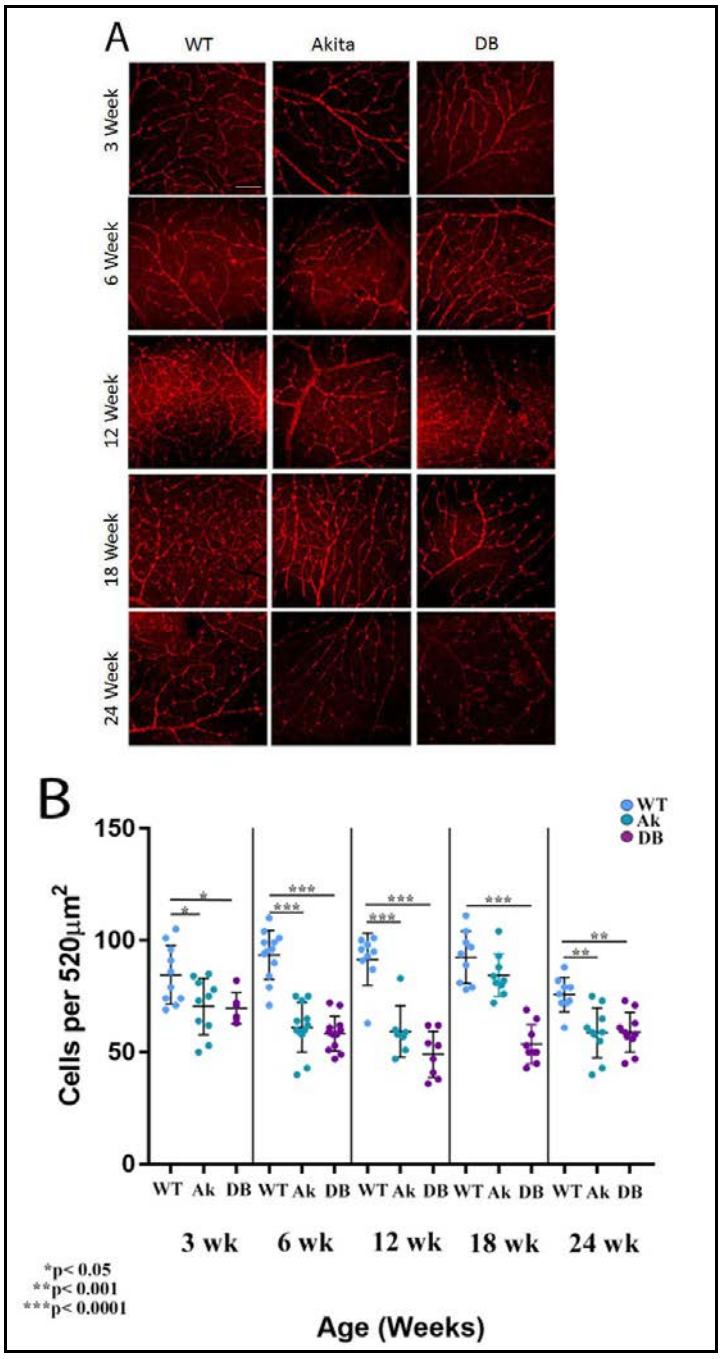


Figure 13 Pre-retinal pericyte numbers decrease in 2 models of DR. A) Retinal flatmounts from 3, 6, 12, 18, and 24 week mice from WT, Akita, and DB mice were immunolabeled with neural/glial antigen 2 (NG2), a pericyte cell marker (Ozerdam et al., 2001). Each retina was subdivided into two regions; 1) the area up to 1500um$^2$ from the optic nerve, or 2) the area from 1500-300um$^2$ from the optic nerve. Within each region, 3-5 counts were taken using NIH image J (Schneider et al., 2012) and the numbers averaged together (N=5 retina/stage/genotype). Magnification bar = 50 μm B) Quantification of NG2$^+$ cells were graphed using the scatter dot plot function of GraphPad Prism with the average and error bars shown in black. Statistical significance were determined using a one-way analysis of variance (ANOVA) with a Tukey's multiple comparison test (* $p<0.05$; ** $p<0.001$; *** $p<0.0001$).

### 3.2 Retinal microvasculature showed changes early in DB model system that correct with time

Generally speaking, neovascularization has been proposed to occur late in the progression of changes that accompany DR in humans and other species (Alistar et al., 2005; Cheung et al., 2005). Neovascularization, if it occurs at all, has been shown to occur very late in both DB and Akita mice (Cheung et al., 2005, Robinson et al., 2012). No studies to date have done a careful quantitative analysis of the retinal microvasculature in a type 1 or a type 2 model of diabetes throughout the development of the disease. To investigate the retinal vasculature, retinal flat mounts from 3, 6, 12, 18 week-old mice were immunolabeled with the endothelial cell marker isolectin B4 (IB4) (Figure 14A). Images of the retina were analyzed for the percentage of the retinal area labeled with IB4 and the number of branches using AngioTool software (Zudaire et al., 2012). In regards to percentage of area covered by $IB4^+$ vasculature, there were significant increases in vessel area in the DB mice at 3 and 6 weeks in comparison to the WT littermate controls (Figure 14B). The percentage of area covered by the $IB4^+$ cells decreased to control levels in the 12 week DB retinas and remained at the same level in the 18 week retinas. In the Akita retina, total area covered by the $IB4^+$ vasculature did not deviate from those of the WT littermates at any of the ages examined (Figure 14B). A quantitative analysis of branching in the DB retina indicated an increase in branching at all time points examined in comparison to WT retinas (Figure 14C). However, the Akita mice had increased branching only at 6 weeks but no increased vascular area or branching at the other time points (Figure 14C).

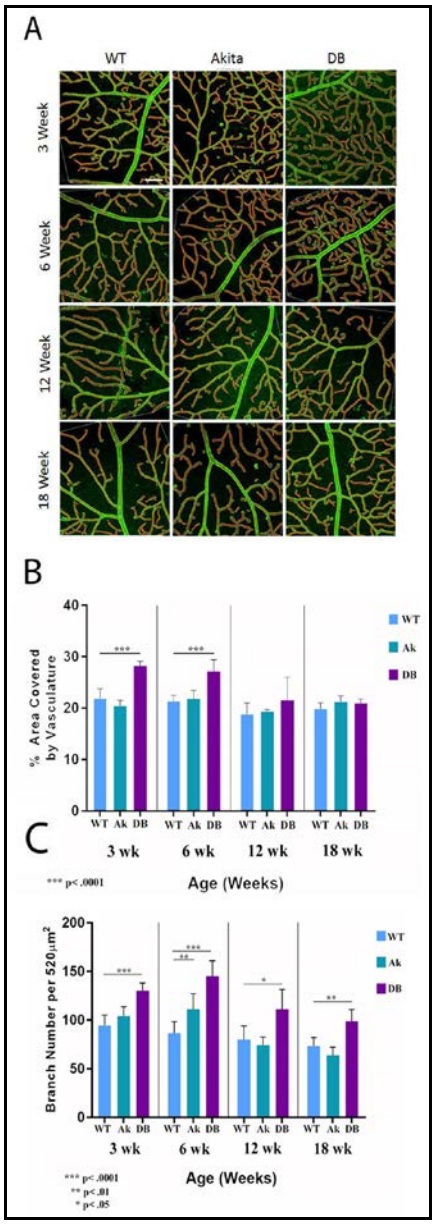


Figure 14. Pre-retinal microvasculature changes occur early in DB model A) Retinal flatmounts at 3, 6, 12, 18, and 24 week WT, Akita, and DB mice were immunolabeled with isolectin B4 (IB4), an endothelial cell marker (Ernst et al., 2006). Magnification bar = 50 µm B) To perform measurements on the retinal vasculature, the retina were again subdivided into two sections (0-1500um$^2$ and 1500-3000um$^2$ from the optic nerve) and the percentage of retinal area covered by vasculature were determined using AngioTool software (Zudaire et al., 2012) (N=4 retinas/stage/genotype). C) Using the same regions of the retina, vascular branch numbers were determined using AngioTool software (Zudaire et al., 2012). Graphs in B and C were plotted using GraphPad Prism and the statistical significance were determined using a one-way ANOVA with a Tukey's multiple comparison test (* p,0.05; ** p< 0.01; *** p<0.0001).

### 3.3 Gliosis was present early in the progression of the disease

In addition to pericyte loss, DR is also accompanied by retinal astrocyte and Müller cell gliosis (Fletcher et al., 2007). Some studies have indicated that gliosis may occur prior to changes in the vasculature (Fletcher et al., 2007, Roque et al., 1990). To determine what stages gliosis might be occurring in each model system in comparison to WT controls, expression patterns of molecules that have been associated with gliosis were examined using RT-qPCR (Dharmarajan et al., 2014 and references therein). As can be seen in Figure 15, mRNA encoding epidermal growth factor receptor (*Egfr*), toll-like receptor 4 (*Tlr4*), phosphacan (*Pcan*), and tissue inhibitor of metalloproteinase 2 (*Timp2*) are upregulated more than 1.5 fold (0.58 in log2 scale) at 3 weeks in the Akita retinas. Increases in gene expression appear to peak at the 12 week time point and are reduced thereafter (Figure 15).

In comparison, some of the gliosis markers, including glutamine synthetase (*Gs*), *Egfr*, neurocan (*Ncan*) and matrix metalloproteinase 14 (*Mmp14*) were actually downregulated in the DB retinas in comparison to control levels (as indicated by levels below 0). By 6 weeks, many markers were expressed at levels well above the controls, including glial fibrillary acidic protein (*Gfap*), *S100b*, vimentin (*Vim*), *Egfr*, *Pcan*, and *Mmp14*. In the DB samples, the gliosis appeared to peak between 6 and 12 weeks, and by 18 the levels were reduced (Figure 16).

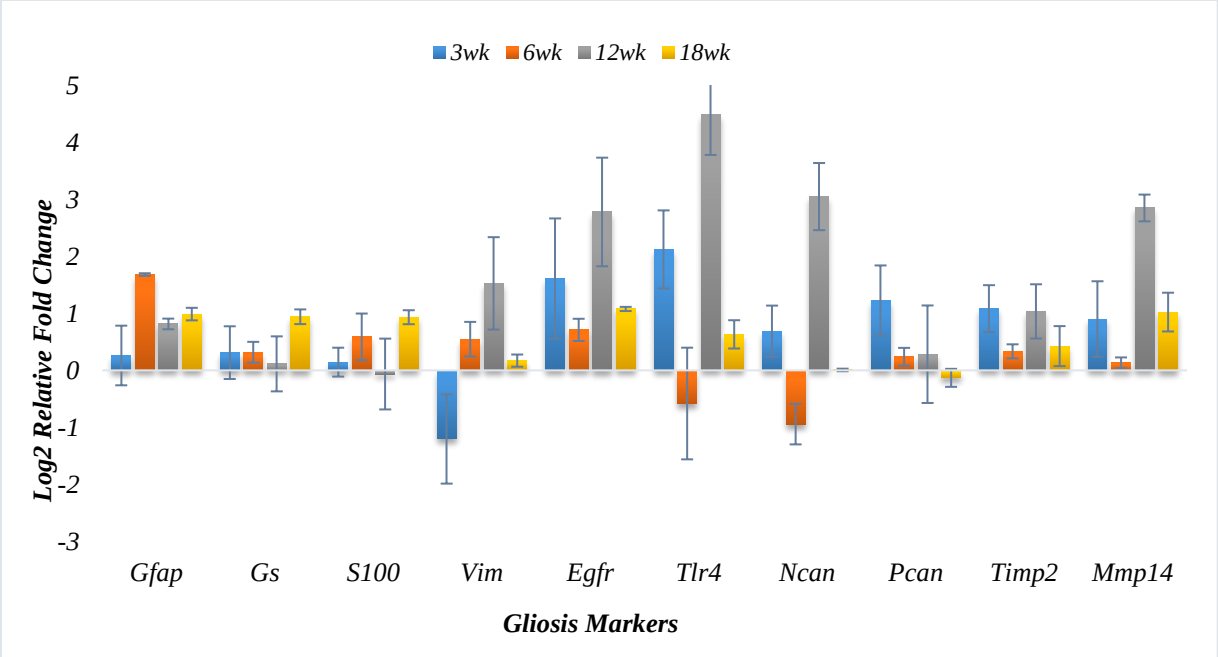


Figure 15 Gliosis in Akita mice increase as early as 3 weeks. Expression levels of a panel of gliosis markers were analyzed by RT-qPCR in RNA samples from retina samples in 3, 6, 12, and 18 week aged mice. Retinas were isolated and 2.5ng of original RNA was used. Quantitation was done using the method by Pfaffl, 2010 (Pfaffl, 2010). Expression levels were normalized to a geometric mean of 3 housekeeping genes, β- 2 Microglobulin (*B2m)*, succinate dehydrogenase complex subunit A (*Sdha*), and signal recognition particle 14 kDa (*SRP14*). RNA levels of Akita mice were compared relative to WT littermates. Bars above a level of (0.58) represent an increase of over 1.5 fold change (significant increase) in mRNA levels while bars below the level of 0 represent a decrease in mRNA levels relative to the corresponding vehicle control. At 3 weeks, there is a significant decrease in *Vim* and *Ncan* while *Mmp14*, *Timp2*, *Tlr4*, and *Egfr*. At the 6 week time point, there is a significant increase in mRNA expression in *Gfap*. At the 12 week mark, many gliosis markers have significant increased expression, with only *S100*, *Gs*, *Pcan*, not showing increased levels when compared to their WT counterparts. At the 18 week mark, there is a decrease in mRNA levels of many markers, although have over 1.5 fold change when compared to their WT counterparts. Abbreviations: *Gfap* glial fibrillary acidic protein, *Gs*-glutamine synthetase, *S100*-calcium-binding protein B, *Vim*-Vimenten, *Egfr*- epidermal growth factor receptor, *Tlr4*-toll like receptor 4, *Ncan*-neurocan, *Pcan*-phosphocan, *Timp2*- tissue inhibitor of matix metalloproteinases 2, *Mmp*- matrix metalloproteinase.

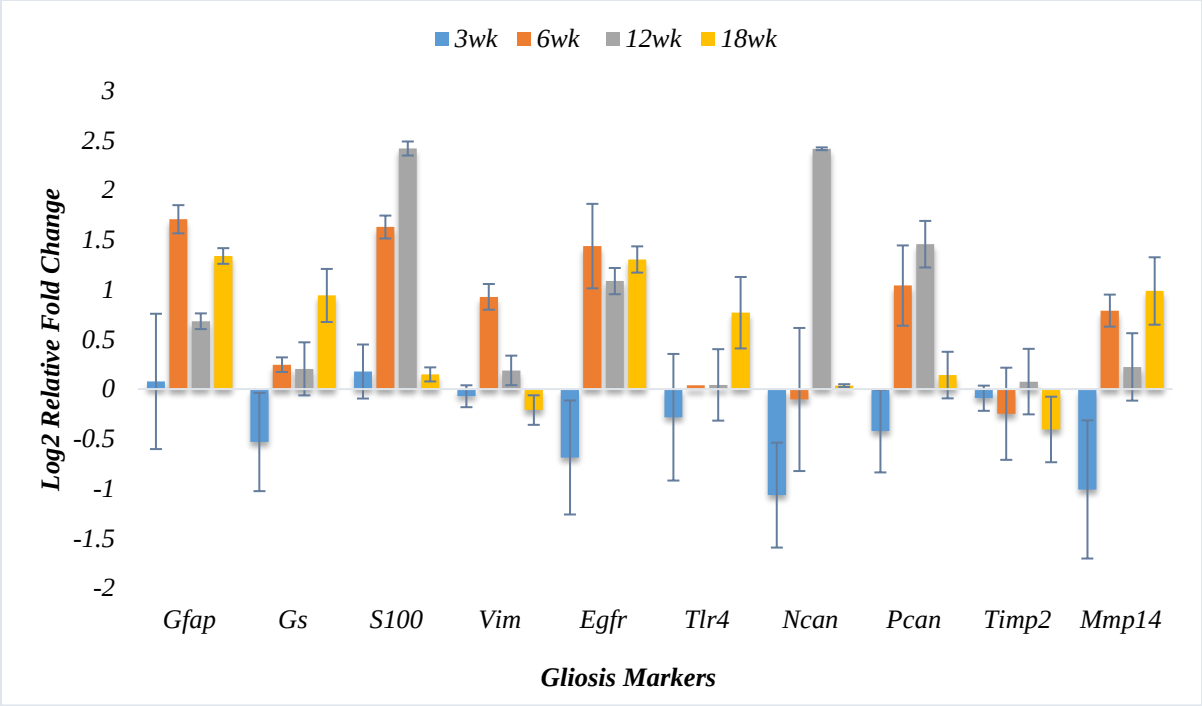


Figure 16 Gliosis in DB mice increase as early as 6 weeks. Expression levels of a panel of gliosis markers were analyzed by RT-qPCR in RNA samples from retina samples in 3, 6, 12, and 18 week aged mice. Retinas were isolated and 2.5ng of original RNA was used. Quantitation was done using the method by Pfaffl, 2010 (Pfaffl, 2010). Expression levels were normalized to a geometric mean of 3 housekeeping genes, β- 2 Microglobulin (*B2m)*, succinate dehydrogenase complex subunit A (*Sdha*), and signal recognition particle 14 kDa (*SRP14*). RNA levels of DB mice were compared relative to WT littermates. Bars above a level of (0.58) represent an increase of over 1.5 fold change (significant increase) in mRNA levels while bars below the level of 0 represent a decrease in mRNA levels relative to the corresponding vehicle control. At 3 weeks, there is a significant decrease in *Ncan* and *Mmp14*. At the 6 week time point, there is a significant increase in mRNA expression in *Gfap, S100, Vim, Egfr, Pcan,* and *Mmp14.*At the 12 week mark, many of these markers stay increased along with *Ncan*, although *Vim* does almost reach WT levels. At the 18 week mark, there is an increase in *Gs* and *Tlr* while *Vim, Ncan,* and *S100* decrease back to the control mRNA levels. Abbreviations: *Gfap* glial fibrillary acidic protein, *Gs*-glutamine synthetase, *S100*-calcium-binding protein B, *Vim*-Vimenten, *Egfr*- epidermal growth factor receptor, *Tlr4*-toll like receptor 4, *Ncan*-neurocan, *Pcan*-phosphocan, *Timp2*- tissue inhibitor of matix metalloproteinases 2, *Mmp*- matrix metalloproteinase.

Proliferation of astrocytes can sometimes accompany gliosis (Sardar et al., 2017; Selmaj et al., 1990). To determine if retinal astrocytes were proliferating in either model, retinal flat mounts from 3, 6, 12, 18, and 24 week DB and Akita retinas were immunolabeled with astrocyte and progenitor marker SOX2 (Figure 17A). Quantitative analysis of astrocyte numbers indicated there was no increase to the number of $SOX2^{+}$ cells in the DB or Akita samples in comparison to WT controls (Figure 17B)

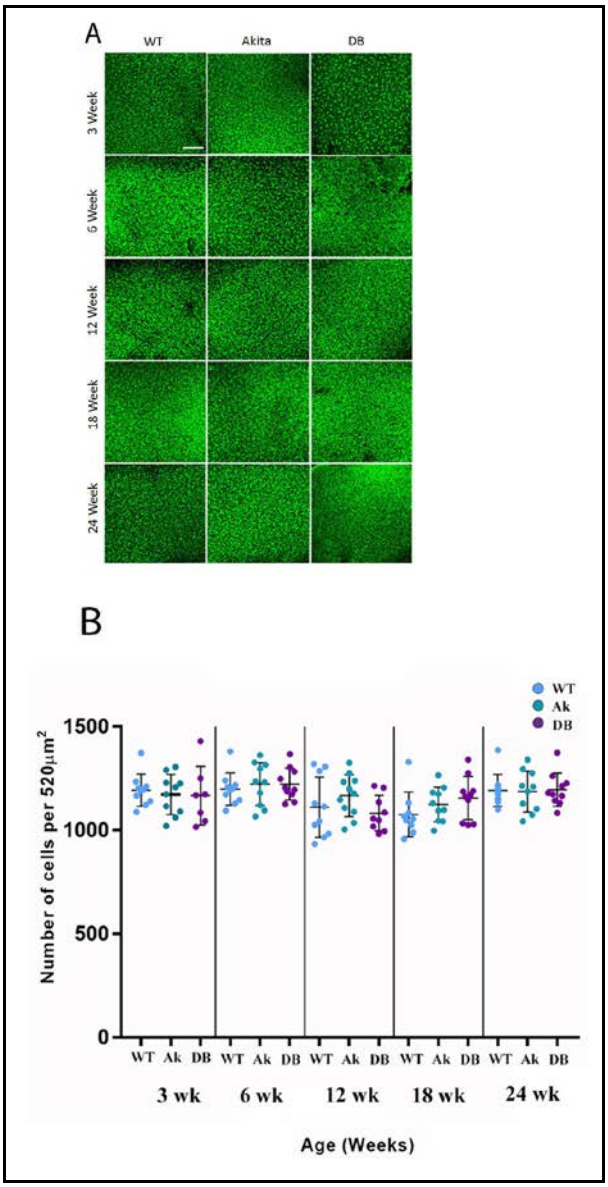


Figure 17 Pre-retinal astrocyte numbers do not change in Akita or DB model system in comparison to WT littermates. A) Retinal flatmounts at 3, 6, 12, 18, and 24 week from WT, Akita, and DB mice were immunolabeled for sex determining region y (SRY) -box 2 (SOX2), an astrocyte and progenitor cell marker (Ellis et al., 2004). Each retina was subdivided into two regions; 1) the area up to 1500um$^2$ from the optic nerve, or 2) the area from 1500-300um$^2$ from the optic nerve. Within each region, 3-5 counts was taken using NIH image J (Schneider et al., 2012) and the numbers averaged together (N=5 retina/stage/genotype). Magnification bar = 50 µm
B) Quantification of SOX2$^+$ cells was graphed using the scatter dot plot function of GraphPad Prism with the average and error bars shown in black. Statistical significance was determined using a one-way analysis of variance (ANOVA) with a Tukey's multiple comparison test.

### 3.4 Proinflammatory mRNA levels are increased as early as 6 weeks in Akita and DB models

Clearly, there are changes to pericyte number in both Akita and DB models by 3 weeks (Figure 16). It is unclear when inflammatory changes occur to the retina of each model system; however, there are known to be increases in proinflammatory markers, particularly at later stages of DR (Tung and Kern, 2011; Tang et al., 2011, Byeon et al., 2010). To determine when increases in proinflammatory markers were present in the retina of Akita and DB models mRNA levels of specific markers were investigated using RT-qPCR at 3, 6, 12, and 18 weeks.

In the Akita retina, pro-inflammatory mRNA levels at the 6 week time point significantly increase in *Csf*, *Ifnγ*, *Il6*, *Vegf*, *Ccl5*, and *Thbs1*. Expression of many those markers increased or stayed at a similar level at the 12 week time point and was joined by increases in *Gmcsf*, *Ifnα*, *Il1β*, *Thbs2*, and *Iba1* (Figure 18). Twelve weeks appears to have been the peak in changes to mRNA levels, thereafter there was a decrease in mRNA levels.

The DB model differed from the Akita model in that several mRNAs appeared to have mRNA levels below that of WT controls at 3 weeks, including *Csf*, *Ifnα*, *Ifnγ*, *Vegf*, and *Thbs1* (Figure 19). At 6 weeks, there were moderate increases in levels of *Ifnα*, *Ifnγ*, *Il1β*, *Vegf*, *Ccl5*, *Thbs1*, and *Iba1*. The mRNAs for the proinflammatory markers appeared to peak around 12-18 weeks (Figure 19). Three markers (*Ifnγ*, *Ccl5*, and *Cd68)* showed a decrease at 12 weeks, followed by an abrupt increase at 18 weeks.

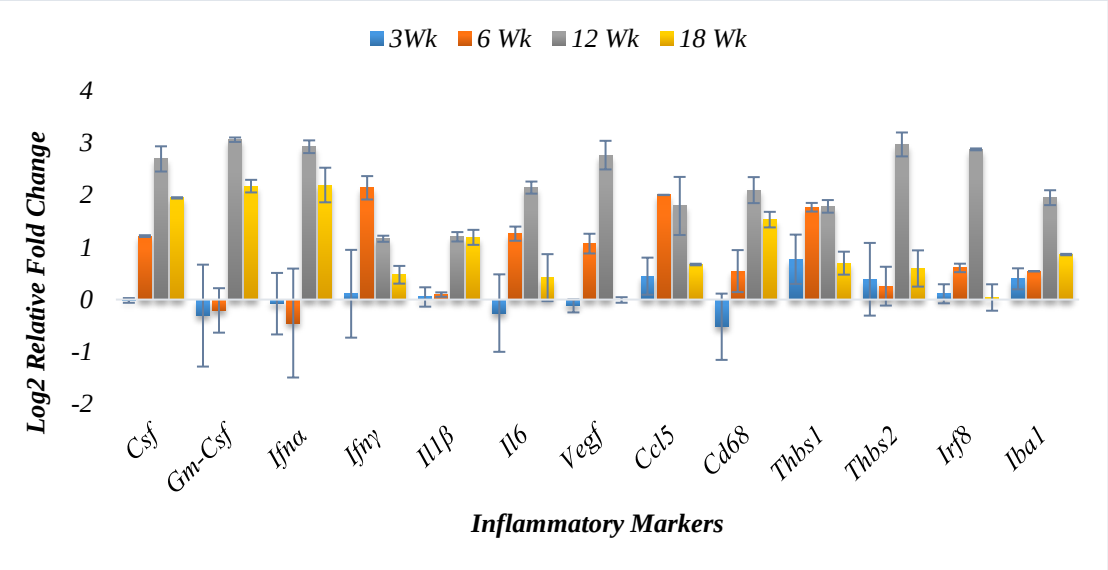


Figure 18 Proinflammatory markers increase at 6 weeks for Akita mice. Expression levels of a panel of inflammatory markers were analyzed by RT-qPCR in RNA samples from retina samples in 3, 6, 12, and 18 week aged mice Akita and WT. Retinas were isolated and 2.5ng of original RNA was used. Quantitation was done using the method by Pfaffl, 2010 (Pfaffl, 2010). Expression levels were normalized to a geometric mean of 3 housekeeping genes, β- 2 Microglobulin (*B2m*), succinate dehydrogenase complex subunit A (*Sdha*), and signal recognition particle 14 kDa (*Srp14*). RNA levels of Akita mice were compared relative to WT littermates. Bars above a level of (0.58) represent an increase of over 1.5 fold change (significant increase) in mRNA levels while bars below the level of 0 represent a decrease in mRNA levels relative to the corresponding vehicle control. At 3 weeks, there no major increases or decrease of proinflammatory mRNA expression. Abbreviations: *CD*; cluster of differentiation, *Csf;*colony stimulating factor, *Gm-csf;* granulocyte macrophage colony stimulating factor, *Ifn*; interferon, *Il;* interleukin, *Tnf-α;* tumor necrosis factor alpha, *Thbs;* thrombospondin, *Vegf;* vascular endothelial growth factor, *Irf;* interferon regulating factor, *Iba1;* ionized calcium-binding adaptor molecule 1.

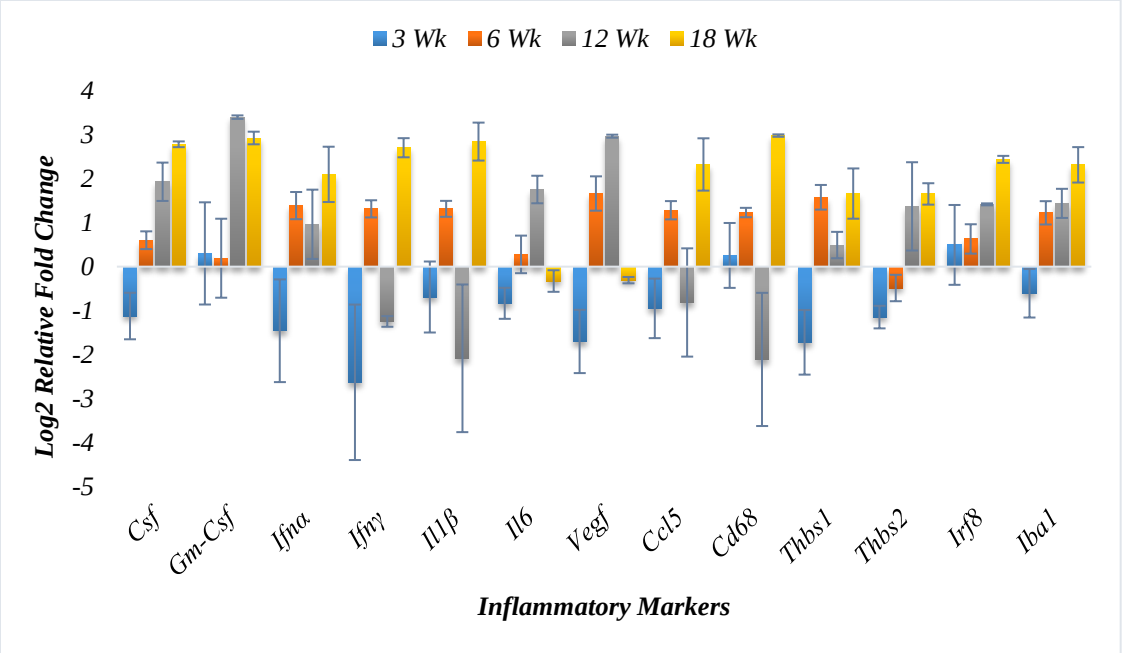


Figure 19 Proinflammatory markers increase at 6 weeks for DB mice. Expression levels of a panel of inflammatory markers were analyzed by RT-qPCR in RNA samples from retina samples in 3, 6, 12, and 18 week aged DB and WT mice. Retinas were isolated and 2.5ng of original RNA was used. Quantitation was done using the method by Pfaffl, *2010* (Pfaffl, 2010). Expression levels were normalized to a geometric mean of 3 housekeeping genes, β- 2 Microglobulin *(*B2m), succinate dehydrogenase complex subunit A *(*Sdha*)*, and signal recognition particle 14 kDa *(*SRP14*)*. RNA levels of DB mice were compared relative to WT littermates. RNA levels of DB mice were compared relative to WT littermates. Bars above a level of (0.58) represent an increase of over 1.5 fold change (significant increase) in mRNA levels while bars below the level of 0 represent a decrease in mRNA levels relative to the corresponding vehicle control. Abbreviations: *CD*; cluster of differentiation, *Csf;*colony stimulating factor, *Gm-csf;* granulocyte macrophage colony stimulating factor, *Ifn*; interferon, *Il;* interleukin, *Tnf-α;* tumor necrosis factor alpha, *Thbs;* thrombospondin, *Vegf;* vascular endothelial growth factor, *Irf;* interferon regulating factor, *Iba1;* ionized calcium-binding adaptor molecule 1.

As tight junctions fail during DR, cells from the immune system have been shown to infiltrate the blood-retinal barrier, and some of those cells are capable of differentiating into macrophage and microglial cells (Streit et al., 1996). To investigate whether any of the changes in mRNA or protein levels of proinflammatory proteins was due to an increase in myeloid lineage cells, retinal flat mounts from Akita and DB mice were immunolabeled at 3, 6, 12, 18, and 24 weeks with antibody specific for myeloid-lineage specific protein IBA1 (Figure 20A). $IBA1^+$ cells were quantified in images taken from these samples (Figure 20B). In the Akita retinas, there were similar numbers of $IBA1^+$ cells in comparison to WT at each age examined;

however, in the DB samples there was a small decrease at 3 weeks, followed by an increase at 12 weeks in comparison to WT retinas (Figure 20B).

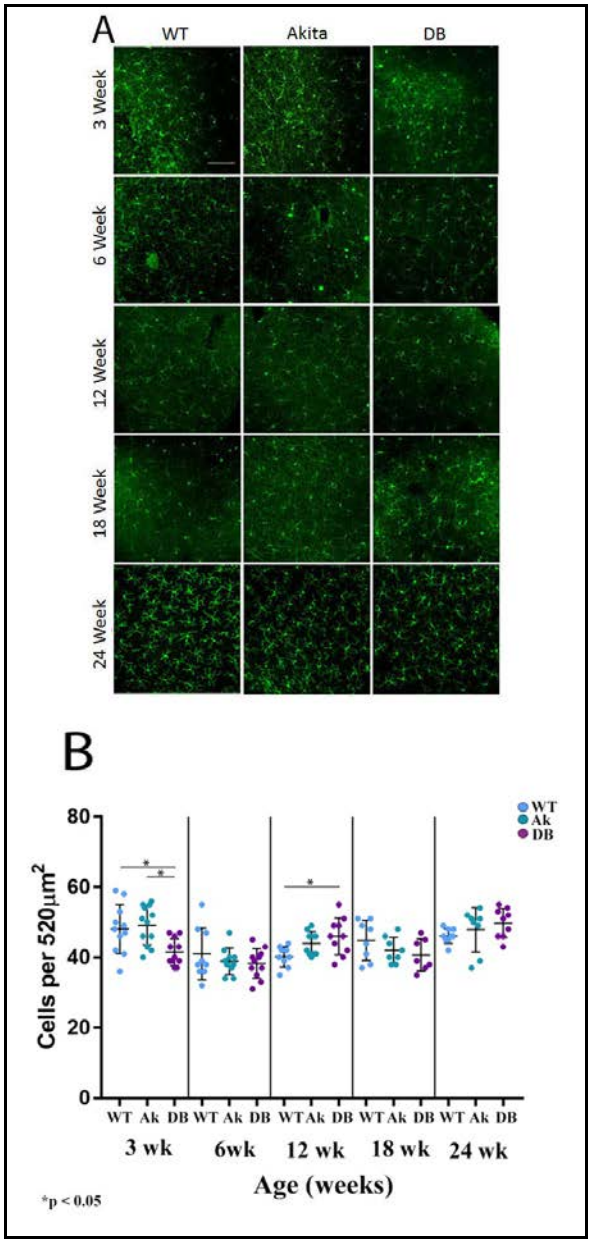


Figure 20 Numbers of pre-retinal IBA1+ microglial cells. A) Retinal flatmounts at 3, 6, 12, 18, and 24 week from WT, Akita, and DB mice were immunolabeled for myeloid lineage marker IBA1 (Ito et al., 1998). Each retina was subdivided into two regions; 1) the area up to 1500um$^2$ from the optic nerve, or 2) the area from 1500-300um$^2$ from the optic nerve. Within each region, 3-5 counts was taken using NIH image J (Schneider et al., 2012) and the numbers averaged together (N=5 retina/stage/genotype). Magnification bar = 50 µm B) Quantification of IBA1$^+$ cells was graphed using the scatter dot plot function of GraphPad Prism with the averageand error bars shown in black. Statistical significance was determined using a one-way (ANOVA) with a Tukey's multiple comparison test (* $p<0.05$).

### 3.5 PDGFRβ signaling is not altered in pericytes acutely treated with IFN-γ.

Our previous results indicated there was an increase in IFN-γ at the mRNA level for Akita and DB models as well as protein levels in the DB model. IFN-γ is of interest for several reasons; 1) it is a potent proinflammatory factor that communicates with cells of the immune system to encourage their infiltration into the nervous system (Feuerer et al., 2006; Singh et al., 1999;), 2) it has been shown to decrease PDGFRβ signaling in human pericytes obtained from epileptic patients (Jansson et al., 2016), and 3) it has been shown to increase activation of PKCδ in some cell types (Deb et al., 2003; Shen et al., 2003). Although a reduction in PDGFRβ signaling and an activation of PKCδ would be consistent with changes described in pericytes of diabetic retinas that lead to apoptosis, neither of these changes have been associated specifically with inflammation in DR.

To investigate whether IFN-γ can trigger changes in survival associated with PDGFRβ signaling and/or PKCδ, isolated pericytes were treated with increasing levels of IFN-γ. Furthermore, we devised a system in vitro in which the effects of acute or chronic exposure to IFN-γ could be tested. In the acute trials, pericytes were treated with various concentrations of IFN-γ for 24 hours, followed by treatment with PDGFBB, while in the chronic trials pericytes were treated with IFN-γ for 72 hours, followed by PDGFBB. This paradigm was used to determine the effect of IFN-γ on PDGFRβ signaling or its downstream pathways. In order to determine differences between total protein levels and activated levels, antibodies specific to the phosphorylated AKT (pAKT), ERK (pERK), and PDGFRβ (pPDGFRβ) along with antibodies specific to the protein AKT, ERK, and PDGFRβ. In the acute treatments, pericytes were treated with 24 hours with 25, 50, and 100ng of IFN- γ and then for 30 mins with 50 ng of PDGFBB (Figure 21, 22, 23). IFN-γ treated pericytes decreased pAKT levels in 1 day treatments as seen

in Figure 21B. At the highest concentration, pAKT activity was decreased. The total protein levels were not changed. Even at early stages of pericyte treatment, IFN-γ decreased the activity of AKT while not changing the total protein levels in the cells. IFN-γ treatment at higher concentration only slightly decreased total PDGFRβ levels but did not change the activity pPDGFRβ levels (Figure 22 B and Figure 22C). Acute IFN-γ treatment increases total ERK levels, but did not change pERK levels (Figure 23B, 23C).

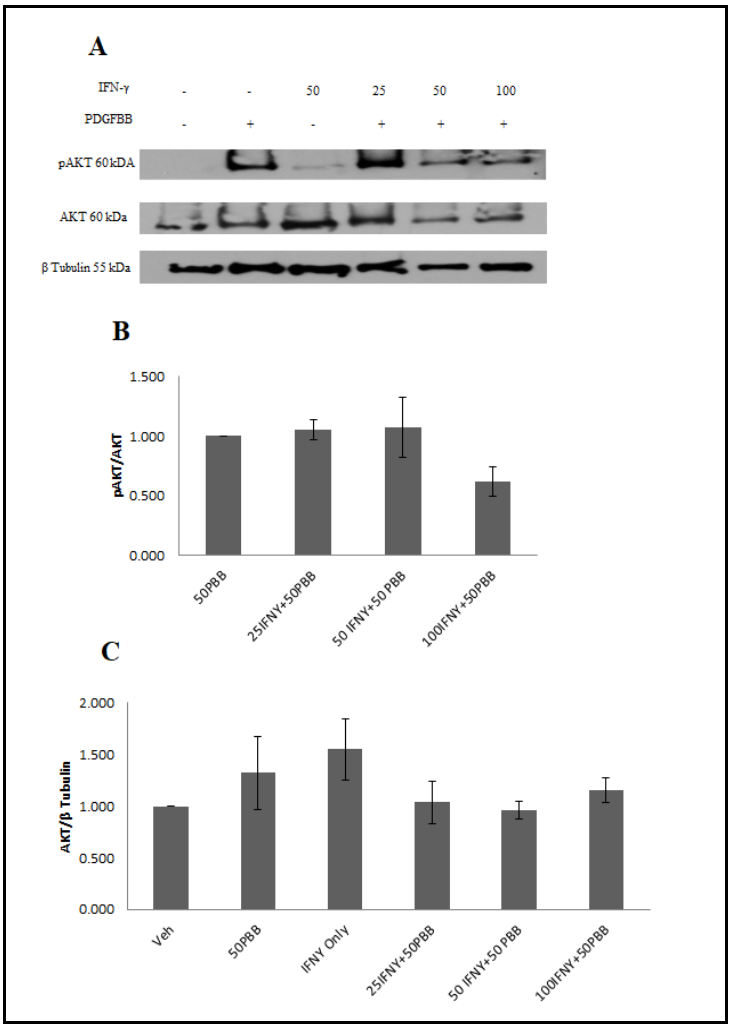


Figure 21 Acute exposure to IFN-γ does not change levels of AKT or pAKt. A) Retinal pericytes were treated for 24 hours with 0 (veh), 25, 50, or 100ng of IFN-γ. After 24 hours of exposure to vehicle or IFN-γ, cells were treated with 50ng of PDGF BB for 30 minutes and protein lysates were examined for levels of pAKT, total AKT, and β tubulin levels (N=3) Densitomeric measurements were performed on the immunoblots using NIH image J (Scheinder et al., 2012). B) Densitometric analysis of pAKT normalized to levels of total AKT. C) Densitometric analysis of AKT normalized to levels of βtubulin. Abbreviations: Veh-Vehicle, PBB- PDGF-BB, IFN-γ-Interferon Gamma, pAKt- phosphorylated AKT.

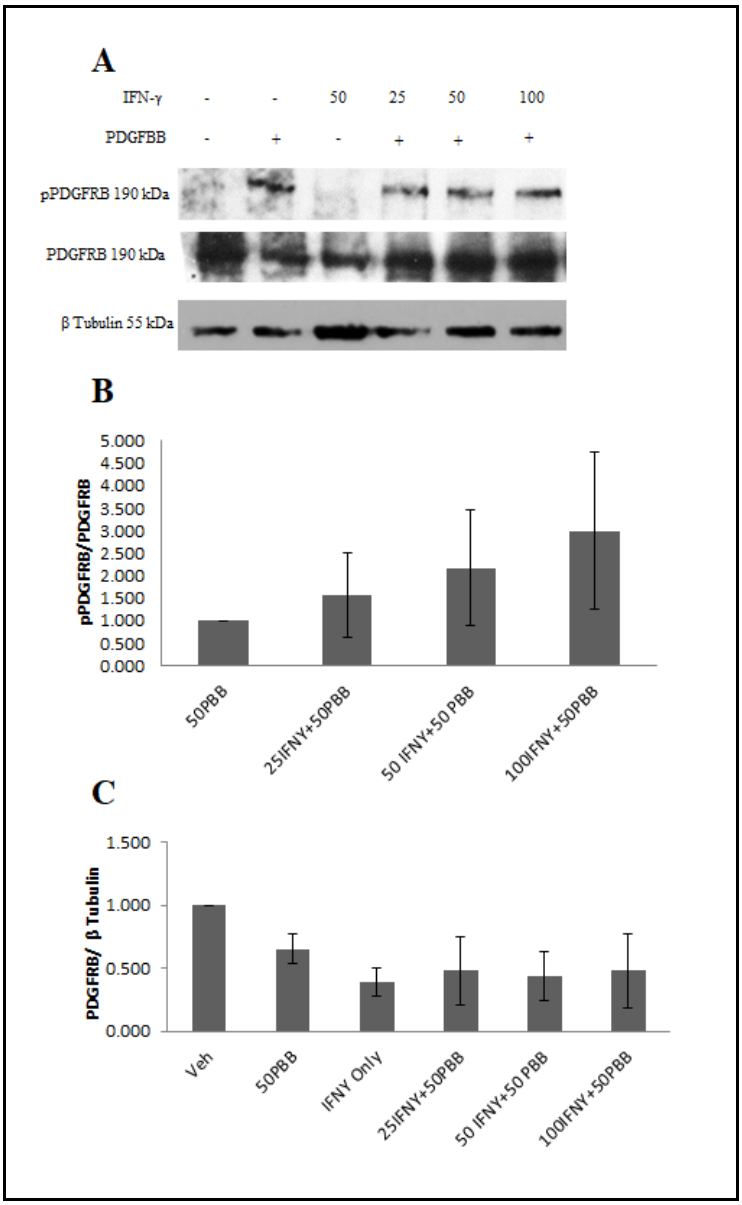


Figure 22 Acute exposure to IFN-γ does not change levels of total PDGFRβ or pPDGFRβ. A) Retinal pericytes were treated for 24 hours with 0 (veh), 25, 50, or 100ng of IFN-γ followed by 30 minute exposure to veh or 50 ng of PDGF-BB. Protein lysates were probed with antibodies specific to pPDGFRβ, total PDGFRβ, or β tubulin. (N=3) Densitomeric measurements were performed on the immunoblots using NIH image J (Scheinder et al., 2012) and the statistical significance was analyzed by one-way ANOVA on the resulting normalized densitometric measurements. B) Densitometric analysis of pPDGFRβ normalized to total PDGFRβ. C) Densitometric analysis of PDGFRβ normalized to β tubulin. Abbreviations: Veh-Vehicle, PBB- PDGF-BB, IFN-γ-Interferon Gamma, PDGFRβ-platelet-derived growth factorβ, pPDGFRβ- phosphorylated platelet-derived growth factorβ.

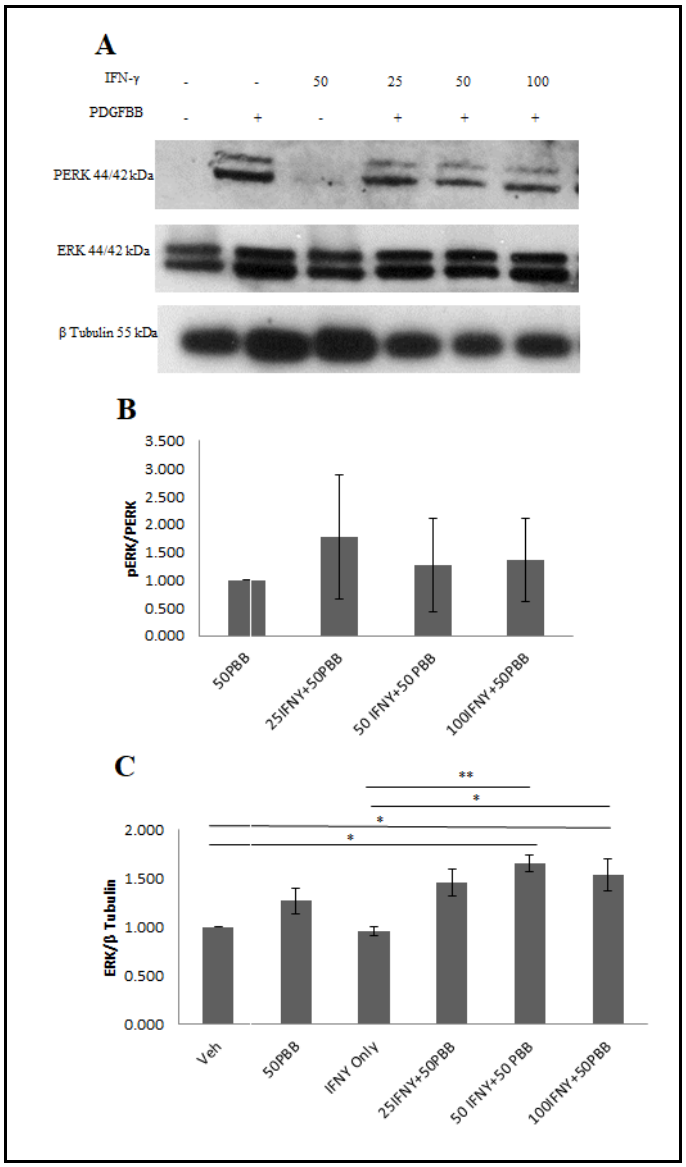


Figure 23 Acute exposure to IFN-γ increases total ERK levels but does not increase pERK levels. A) Retinal pericytes were treated for 24 hours with 0 (veh), 25, 50, or 100ng of IFN-γ followed by 30 minute exposure to veh or 50 ng of PDGF-BB. Protein lysates were probed with antibodies specific to pERK, total ERK, or β tubulin (N=3). Densitomeric measurements were performed on the immunoblots using NIH image J (Scheinder et al., 2012) and the statistical significance was analyzed by one-way ANOVA on the resulting normalized densitometric measurements. B) Densitometric analysis of pERK normalized to total ERK. C) Densitometric analysis of total ERK normalized to β tubulin. (* $p < 0.05$; **$p < 0.01$). Abbreviations: Veh-Vehicle, PBB- PDGF-BB, IFN-γ-Interferon Gamma, ERK-extracellular signal-regulated kinases, pERK- phosphorylated ERK.

### 3.6 pAKT levels were decreased following chronic treatments with IFN-γ

Diabetes can cause a chronic inflammatory state and this can cause angiogenesis seen in DR (Dandona et al., 2003; Jackson et al., 1997). It has also been shown that chronic inflammation have produce different responses can acute inflammation (Gabay and Kushner, 1999; Byeon et al., 2010). Even though there was very little change in the activity and amount of protein expression PDGFRβ or the downstream targets of ERK and AKT, there has been studies done that have shown in chronic conditions IFN-γ does affect PDGFRβ (Jannsson et al., 2016). In order to mimic chronic conditions, pericytes were treated with IFN-γ instead every 24 hours for a total of 72 hours of 1, 25, and 50 ng. PDGFBB was then added for 30 mins and the cells were collected for protein analysis (Figure 24, 25, 26). PDGFRβ, AKT and ERK, both total protein levels and active protein levels were looked at to see if the chronic IFN-γ treatments had different effects than the acute treatments.

pAKT signaling significantly decreased in chronic IFN-γ treatment as seen in Figure 25, unlike the acute conditions. In the 1 and 25 ng chronic IFN-γ treatments with PDGF-BB there was very little change in pAKT signaling at 1 and 25 ng levels, but in the 50 ng IFN-γ and PDGFBB there was a significant decrease in AKT activity when compared to the PDGF-BB treated pericytes alone. There were no changes in normal protein expression levels across the treatments, however, as seen in Figure 24B suggesting that IFN-γ only changes activity of the receptor.

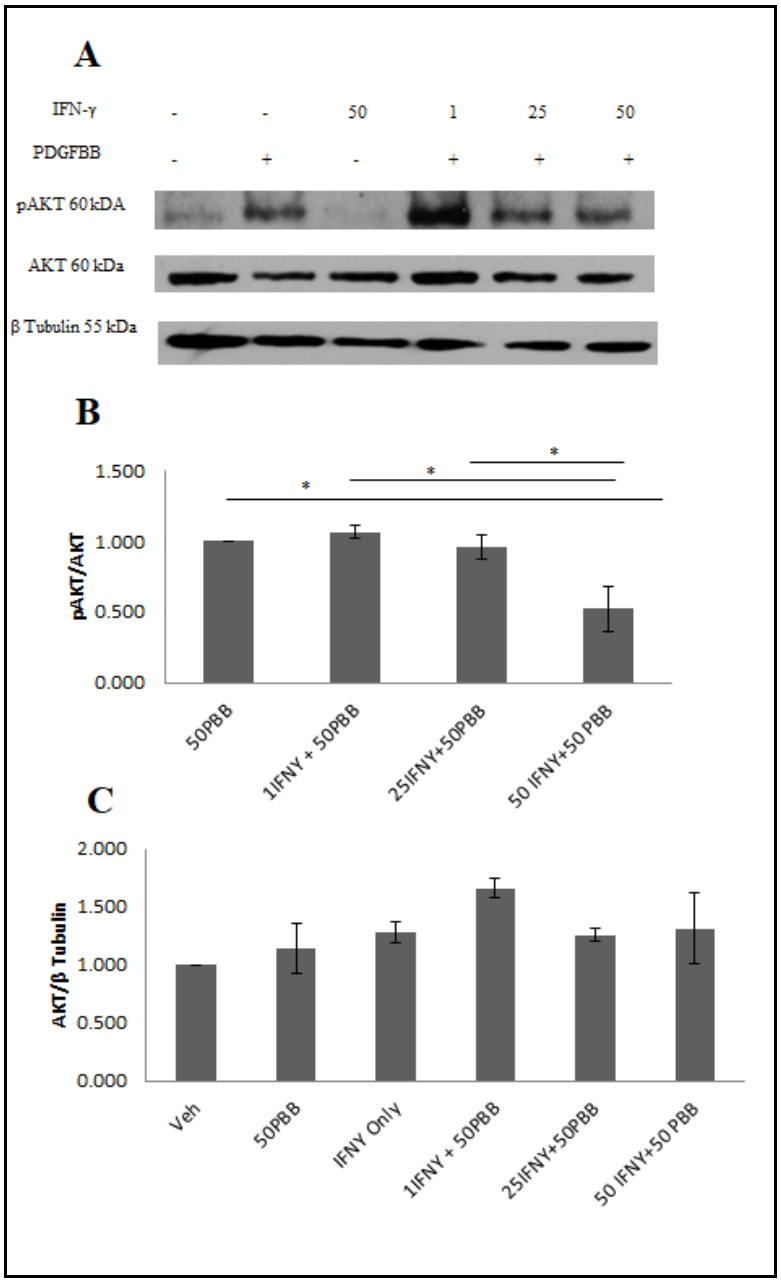


Figure 24 Chronic exposure to high levels of IFN-γ decreases levels of pAKT. A) Retinal pericytes were treated for 72 hours with 0, 1, 25, or 50ng of IFN-γ. After 72 hours of exposure to vehicle or IFN-γ, cells were treated with 50ng of PDGF BB for 30 minutes and protein lysates were examined for levels of pAKT, total AKT, and β tubulin levels. (N=3) Densitomeric measurements were performed on the immunoblots using NIH image J (Scheinder et al., 2012) and the statistical significance was analyzed by one-way ANOVA on the resulting normalized densitometric measurements. B) Densitometric analysis of pAKT normalized to levels of total AKT. (* $p < 0.05$) C) Densitometric analysis of AKT normalized to levels of βtubulin. Abbreviations: Veh-Vehicle, PBB- PDGF-BB, IFN-γ-Interferon Gamma, pAKt- phosphorylated AKT.

### 3.7 PDGFRβ and ERK signaling do not change following chronic treatment with IFN-γ

pPDGFRβ expression did not change in chronic IFN-γ treatments as seen in Figure 25B. There was a slight but statistically insignificant decrease in total PDGRβ seen Figure 25C but the activity of the protein did not change. IFN-γ treatments chronically, like the acute treatments, did not change the activity of the receptor or amount of receptor.

There was also no change in pERK or normal ERK expression levels in chronic treatments as seen from Figure 26 B and C. The addition of IFN-γ and PDGF-BB did not change the total or phosphorylated protein expression in pericytes.

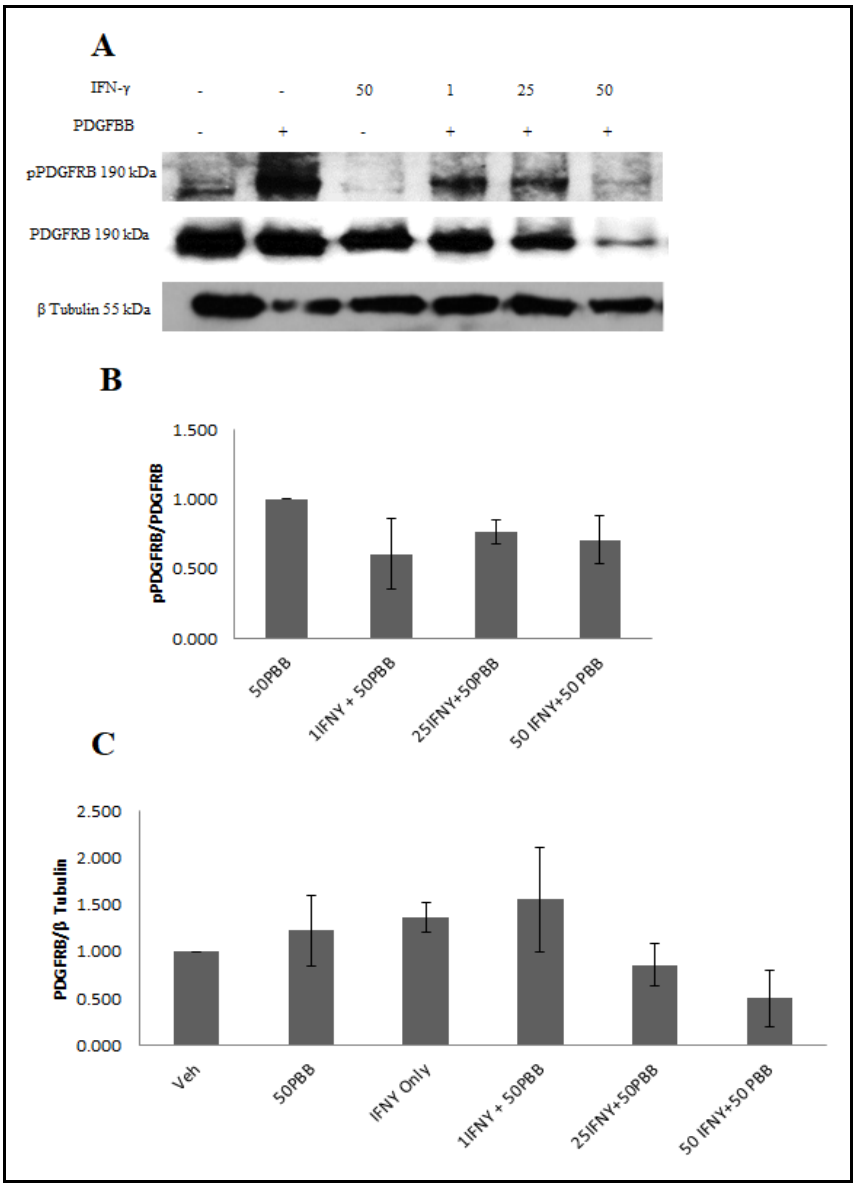


Figure 25 Chronic exposure to IFN-γ does not change levels of total PDGFRβ or pPDGFRβ. . A) Retinal pericytes were treated for 72 hours with 0 (veh), 25, 50, or 100ng of IFN-γ followed by 30 minute exposure to veh or 50 ng of PDGF-BB. Protein lysates were probed with antibodies specific to pPDGFRβ, total PDGFRβ, or β tubulin. (N=3) Densitomeric measurements were performed on the immunoblots using NIH image J (Scheinder et al., 2012) and the statistical significance was analyzed by one-way ANOVA on the resulting normalized densitometric measurements. B) Densitometric analysis of pPDGFRβ normalized to total PDGFRβ. C) Densitometric analysis of PDGFRβ normalized to β tubulin. Abbreviations: Veh-Vehicle, PBB- PDGF-BB, IFN-γ-Interferon Gamma, PDGFRβ-platelet-derived growth factorβ, pPDGFRβ- phosphorylated platelet-derived growth factorβ.

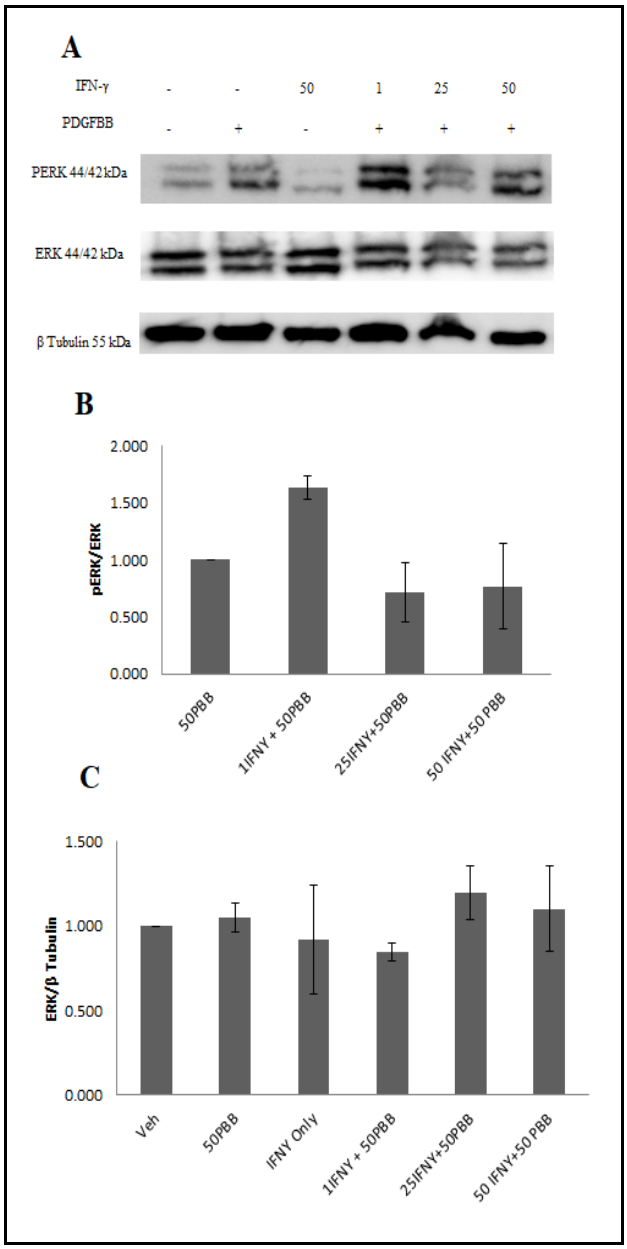


Figure 26. Chronic exposure to IFN-γ does not change levels of ERK or pERK. A) Retinal pericytes were treated for 72 hours with 0 (veh), 25, 50, or 100ng of IFN-γ followed by 30 minute exposure to veh or 50 ng of PDGF-BB. Protein lysates were probed with antibodies specific to pERK, total ERK, or β tubulin (N=3). Densitomeric measurements were performed on the immunoblots using NIH image J (Schneider et al., 2012) and the statistical significance was analyzed by one-way ANOVA on the resulting normalized densitometric measurements. B) Densitometric analysis of pERK normalized to total ERK. C) Densitometric analysis of total ERK normalized to β tubulin. Abbreviations: Veh-Vehicle, PBB- PDGF-BB, IFN-γ-Interferon Gamma, ERK-extracellular signal-regulated kinases, pERK- phosphorylated ERK.

### 3.8 IFN-γ induces PKCδ cleavage in chronic treatments

Increased levels of active PKCδ in relation to DR have been described by other investigators (Geraldes and King, 2010). However, increased PKCδ activity was not assessed at early stages of DR when pericytes were undergoing apoptosis (Geraldes and King, 2010), and no inflammatory pathways have been specifically connected to the rise in PKCδ activity. There is some evidence that IFN-γ can increase PKCδ activity in some cells (Uddin et al., 2002, Gumina et al., 1991); however it has not been investigated in pericytes. PKCδ has been found to be activated in hyperglycemic conditions and negatively regulates AKT activity (Li et al., 2006; Robinson et al., 2012). PKCδ increases SHP-1 activity, which can in turn dephosphorylate ERK, AKT, and even PDGFRβ (Geraldes et al., 2009). To determine if IFN-γ treatment can alter either total PKCδ levels or levels of active PKCδ, pericytes treated chronically with 1, 25, or 50ng of IFN-γ followed by vehicle or PDGFBB. Protein lysates were then investigated using an antibody which will recognize the full c-terminus of the length protein as well as the cleaved activated form of the protein PKCδ (Oh et al., 2004). There is an increase in both total PKCδ levels and cleaved PKCδ when IFN-γ is added in chronic conditions as seen from Figure 27.

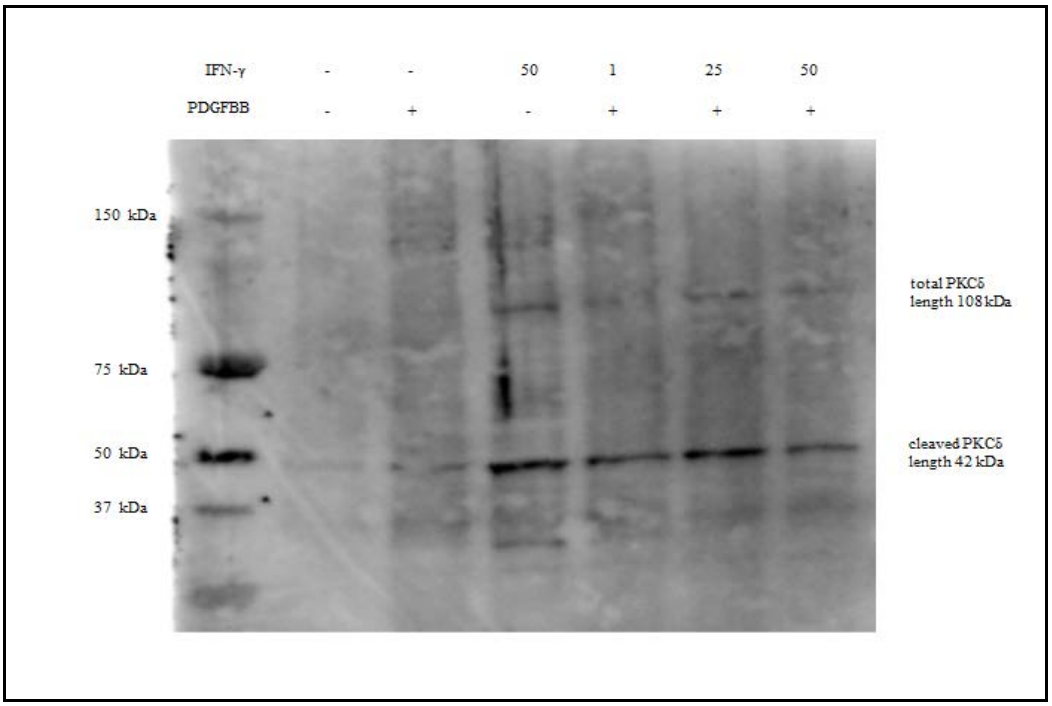


Figure 27 Levels of PKCδ appear to increase following chronic exposure to IFN-γ. Pericytes were treated for 72 hours with 0 (veh), 1, 25, or 50 of IFN-γ followed by 30 minute exposure to vehicle or 50 ng of PDGF-BB. Protein lysates were immunoblotted and probed for antibodies specific for PKCδ. Abbreviations: Veh-Vehicle, PBB-PDGF-BB, IFN-γ-Interferon Gamma.

### 3.9 IFN-γ increased cell death in pericytes without affecting division

Hyperglycemia has been found to decrease survival and increase cell apoptosis in other cell types (Inge et al., 2010; Krankel et al., 2005). This would be consistent with our chronic condition data. Under chronic conditions, pericytes displayed both increased PKCδ activity and decreased AKT phosphorylation, without affecting PDGFRβ or ERK activity or levels. There was also increased cleaved PKCδ levels in chronic conditions. Active caspase 3 cleaves PKCδ while also being a regulator in apoptosis activity (Porter et al., 1999; Basu, 2003). AKT can both upregulate proliferation signaling and downregulate apoptotic signaling (Brunet et al., 2001). Proliferating cell nuclear antigen (PCNA) is a protein that has been associated with active proliferation (Hall et al., 1990). To determine whether there were changes to proliferation and/or apoptosis, pericytes treated chronically with 1, 25, or 50ng of IFN-γ followed by vehicle or PDGFBB. Pericyte were then labeled using an antibody specific for proliferating cell nuclear antigen (PCNA) or cleaved caspase 3.

From Figure 28, there was no change in the percentage of PCNA cells with the addition of PDGF-BB or IFN-γ. IFN-γ or PDGF-BB does affect proliferation in pericytes in chronic conditions. From Figure 29, there was significant increases in cleaved caspase 3 activity in IFN-γ treatments. As the amount of IFN-γ increased, so does the amount of caspase $3^+$ cells. At 1ng IFN-γ treatment, approximately 5% cells displayed active caspase 3 but, at the 50ng IFN-γ this number jumps to 15%. PDGF-BB does not affect caspase 3 activity, as there are no differences in PDGF-BB with IFN-γ or IFN-γ without PDGF-BB.

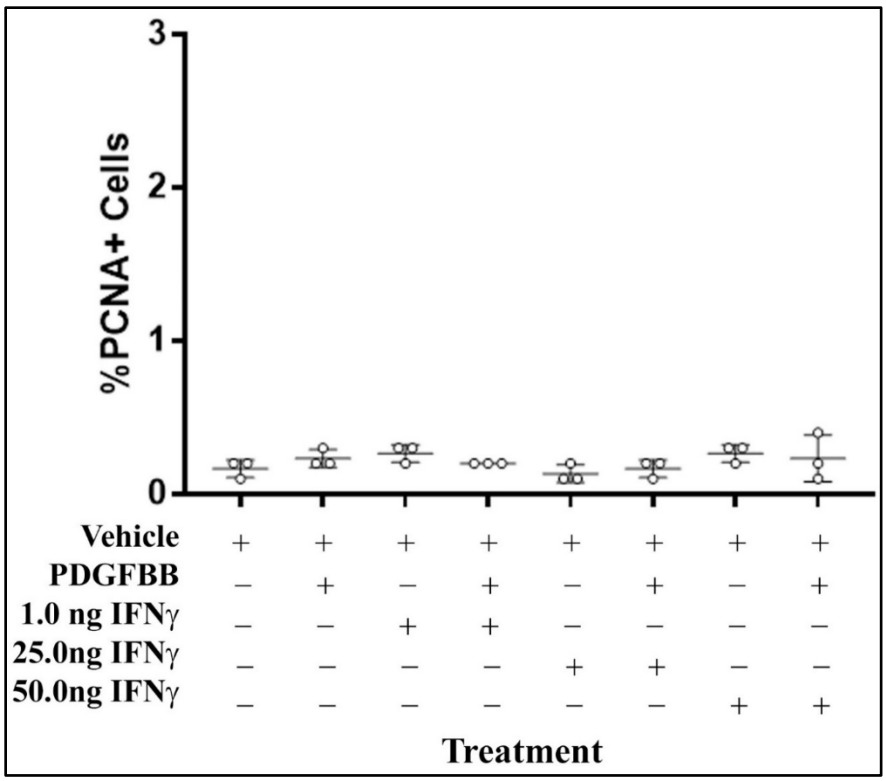


Figure 28 PCNA activity does not change with IFN-γ treatment. Pericytes were treated for 72 hours with 0 (veh), 1, 25, or 50 of IFN-γ followed by 30 minute exposure to vehicle or 50 ng of PDGF-BB. Cells were collected then immunolabeled with PCNA (N=3). Percentage of $PCNA^{+}$ cells over total cells was graphed using the scatter dot plot function of GraphPad Prism with the average and error bars shown in black. Statistical significance was determined using a one-way analysis of variance (ANOVA) with a Tukey's multiple comparison test (* $p<0.05$; ** $p<0.001$; *** $p<0.0001$).

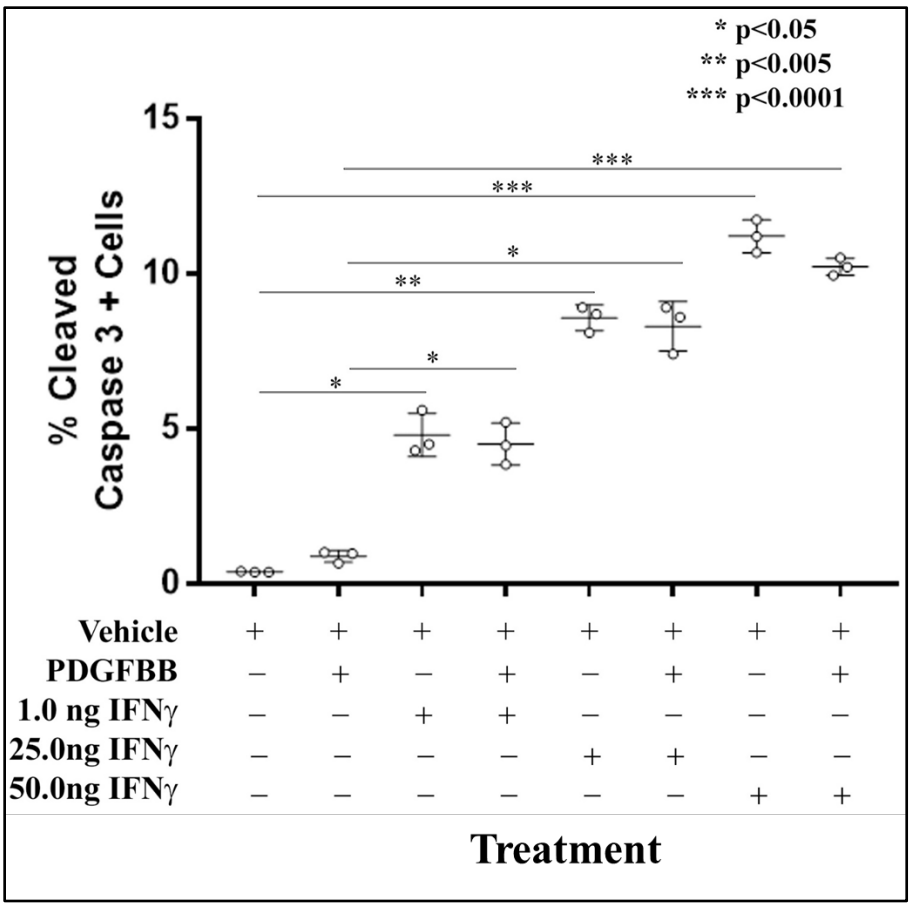


Figure 29 Cleaved caspase 3 activity increased with the addition of IFN-γ. Pericytes were treated for 72 hours with 0 (veh), 1, 25, or 50 of IFN-γ followed by 30 minute exposure to vehicle or 50 ng of PDGF-BB. Cells were collected then immunolabeled with cleaved caspase 3 (N=3). Percentage of cleaved caspase $3^+$ cells over total cells was graphed using the scatter dot plot function of GraphPad Prism with the average and error bars shown in black. Statistical significance was determined using a one-way analysis of variance (ANOVA) with a Tukey's multiple comparison test (* $p<0.05$; ** $p<0.001$; *** $p<0.0001$).

# 4. DISCUSSION

## 4.1 Summary

In the two mouse models, there are several early changes that have not been shown in the literature. Pericyte loss was evident as early as 3 weeks in both mouse models and there was changes in retinal vasculature of DB mice as early as 3 weeks and at 6 weeks in the Akita mice. Gliosis was present in the early progression of diabetes and many of the proinflammatory markers increase as early as 6 weeks. There were no substantial proliferation changes in astrocytes and microglia, although there were increases in activity level.

IFN-γ appeared to regulate apoptosis in isolated pericytes without regulatory mitosis. The increase in apoptosis revolved around an increase in active levels of cleaved PKCδ. At higher levels, the active cleaved PKCδ increased apoptosis by reducing the activity of AKT; however, there were no changes in the activity of ERK or PDGFRβ. Lastly, changes in PCKδ and AKT were seen in chronic IFN-γ conditions, but not following acute treatments.

## 4.2 Two diabetic models display different disease progression

The two diabetic models have different patterns of DR disease progression. Although both mouse models have increased hyperglycemia as early as 4 weeks, the Akita mice are not obese compared to their WT counterpart throughout their lifespan while DB, even at 3 weeks, weigh more. The Akita models have decreased insulin in the blood (hypoinsulinemia) while, DB mice have increased insulin levels (hyperinsulinemia) (Yoshioka et al., 1997; Coleman, 1978). Insulin can contribute to differences seen in the reactivity of different glial cells (Gardner et al., 2002; Villacampa et al., 2013; Haurigot et al., 2009).

Both the DB and Akita mice show a decreased pericyte count as early as 3 weeks and these numbers remain at control levels. There seems to be a recovery of pericytes numbers at 18 weeks for the Akita mice, followed by a reduction in pericyte numbers at 24 weeks. The early 3 week decrease could be caused by either pericyte apoptosis or decreased pericyte recruitment signaling from the neural crest. Inflammation changes at 12 and 18 weeks in the Akita mice could allow for proliferation in pericyte numbers at 18 weeks. At the 12 week mark in the Akita mice, there are marked increases in ECM molecules like NCAN and MMP14, growth factors like CSF and GM-CSF, increase in recruitment molecules like CCL5, and an in regulatory factors like IRF8. There is increased gliosis in Müller glia, microglia, and astrocytes, without a corresponding increase in cell numbers of macroglia (Müller glia and astrocytes) and microglia. This increase in activity, along with the release of growth factors, has been shown to increase signaling in progenitor's cells and cause proliferation of astrocytes and endothelial cells (Burda and Sofronview, 2014).

The differences in pericyte loss along with changes in glial activty could explain why the two models have differences in vascular structure as well. The decreased pericyte number throughout DB mice would correlate with the increased branching and some early vasculature area. Pericytes are important for the stabilization and maintenance of the retinal vasculature and their loss could result in enlarged vessels and decreased stability of these vessels, as shown from the increased branches and vasculature changes in early stage DB mice (Hellstrom et al., 2001; Sweeney et al., 2016; Bergers and Song, 2005). As the DB mice age, there might be some compensatory mechanism that helps restore vasculature area. The Akita mice only show significant branching at the 6 week mark could mean that obesity and/or the underlying metabolic disorder plays a major difference in vasculature changes.

In the two mouse models, there are few changes in microglia and astrocyte numbers, but there is significant change in astrocyte and microglia activity. There are however, small changes in microglia numbers as DB mice have increased microglia at 12 week and a decrease at 3 week while the Akita mice show no changes in microglia number at all. Activated microglia enhance phagocytosis, proliferation, migration, and can induce release of cytokines like TNFs, IL-6 (Langmann, 2007). This is consistent with the increased mRNA levels *Cd68* and *Iba1* along with *Tlr4* and *Il6*.

There are very important changes seen in DB mice that have not been the described in literature in pericytes. Most pericyte loss and vascular changes in DB mice have been shown to occur at 6 months stage, while in our study there are changes as early as 3 weeks (Linwincz et al., 1990; Chou et al., 2014). There is a decrease in mRNA levels of ECM molecules, *Mmp14* and *Ncan* at early stages and a decrease in many proinflammatory markers like *Ifnγ*, *Il6*, and *Vegf*. This would suggest that DB mice have an anti-inflammatory environment early in their life. It has been shown in other models that a lack of leptin function can impair immunity, through a decreased spleen and thymus function (Wellen and Hotamisligil, 2005). Starting at 6 weeks, after hyperglycemia and obesity start to increase, there is an increase in proinflammatory markers and some gliosis markers. At 12 and 18 weeks, there is a significant increase in the mRNA levels of proinflammatory and gliosis markers. The increase in activity in other cells can cause changes associated with inflammation (Burda and Sofronview, 2014).

In the Akita mice, there are differences in disease progression in comparison to DB mice. Even though there is a decrease in pericyte numbers as early as 3 weeks, there is no corresponding vasculature change at 3 weeks. There is also pericyte recovery at 18 weeks, which was not seen in the DB mice. The inflammation pattern is very similar to DB mice after

hyperglycemia initiates, as there is an increases in many proinflammatory markers at 6 weeks. There is a concomitant increase in mRNA levels of gliosis markers at 12 weeks. This evidence suggests that glucose level is not the only factors influencing the pathology of DR, but obesity may also play a role.

### 4.3 Downstream effects of PDGFRβ changed in IFN-γ treatments

In the in-vivo studies of pro-inflammatory markers, we determined that there was an increase in IFN-γ mRNA and protein. Further studies were focused on the role of IFN-γ in pericyte survival. PDGF-BB treatment activates PDGFRβ and causes activation of ERK and AKT, which was used as our positive control (Chaudhary and Hruska, 2001). There were some major differences in acute treatments and chronic treatments in affecting PDGFRβ signaling. Both treatments had small but statistically insignificant decreases in overall PDGFRβ expression, though the activity of the receptor did not appear to change measurably. In the chronic treatments; however, there is decreased levels of pAKT, while the pAKT levels in the acute treatments did not appear to change. High levels of IFN-γ appear to cause an increase in apoptosis, specifically using the P13K/AKT pathway as there was no change in ERK signaling in both the chronic and acute conditions. There is an increase in the overall ERK levels at the acute treatment was not present following chronic treatment with IFN-γ.

The acute phase increase in overall ERK expression with the lack of change in phosphorylation suggests the cells could be undergoing apoptosis. While AKT has been found to be very anti-apoptotic, ERK has been found to be activated in both survival and apoptosis. ERK signaling promotes anti-apoptotic proteins, such as B-cell lymphoma 2 (BCL-2), myeloid leukemia cell differentiation protein (MCL-1), inhibitor of apoptosis (IAP) and represses pro-apoptotic proteins, BAD and BCL-2-like protein 11 (BIM) (Cagnol and Chambard, 2009).

However, ERK has also been shown to activate apoptosis through caspase-8 activation or cytochrome c release (Cagnol and Chambard, 2009).

It has been found that hyperglycemia does increase activation of both SHP-1 and and PKCδ (Geraldes et al., 2009). SHP-1, a well-known phosphatase, can negatively regulate AKT, ERK, and PDGFRβ signaling under some circumstances; however, we did not detect a measurable change in pERK or pPDGFRβ (Lodeiro et al., 2011). PKCδ and AKT have been shown to regulate each other in other models (Li et al., 2006; Gao et al., 2008, Tanak et al., 2003). The activity and even amount of PKCδ was increased as IFN-γ was added in our pericytes. PKCδ has been shown to increase apoptosis its nuclear translocation and subsequent activation of p53 and release of cytochrome c (Coutinho et al., 2009). The release of cytochrome c increases cleavage and activity of caspase 3, which was seen in the chronic IFN-γ treatments (Liu et al., 2015). Cell proliferation; however, was not affected by chronic IFN-γ treatment. This suggests that inflammation does play a role in pericyte cell death, similar to what Jansson et al. found in their study (2016). However, Jansson et al. found a decrease in PDGFRβ, AKT, and ERK signaling which we did not detect (2016). This could be due to a couple of reasons. Animal models of diseases progress differently than humans as mouse models have not been found to fully replicate chronic human inflammatory diseases (Seok et al., 2013). The pericytes used by Jansson et al. were isolated from human patients with epilepsy while our pericytes were from obtained from a diabetic mouse model (2016). Epilepsy can induce changes like increased pericyte loss, changes in astrocyte and endothelial cells, and changes in inflammation itself (Vezzani et al., 2005; Liwnicz et al., 1990; Heinemann et al., 2012).

### 4.5 Future Directions

IFN-γ specifically activates the janus kinase (JAK) and signal transducers and activators of transcription (STAT), specifically JAK 1 and JAK2 into STAT1. JAK1 and JAK2 along with STAT1 should be furthered studies to see the effects of their roles in apoptosis, PKCδ, and PDGFRβ in pericytes IL-6 treatments should be done to see if this apoptosis and AKT signaling is STAT-1 specific or if STAT3 and other STAT's can also produce similar results (Rawlings et al., 2004). Other growth factors involved in angiogenesis, like VEGF, can also be looked at to see if this pathway is similarly affected. IFN-γ, as found in our study, does not directly affect PDGFRβ signaling, but it does affect PKCδ and AKT activity. There could be other pathways that IFN-γ affects that were not examined. TNF-α has been shown to interact with IFN-γ (Gabay et al., 1999; Loddenkemper et al., 2006; Tilg et al., 1994). A combination of different pro-inflammatory factors, like TNF-α with IFN-γ, in PDGFRβ signaling in pericytes as well as pericyte survival.

In-vivo studies may not have the same effect as in-vitro studies. PDGFRβ signaling in both animal models should be looked at in-vivo to see if similar results as seen by in-vitro results. Pericyte loss should be further examined in 3 week mice to determine the exact cause. Cytochrome c and caspase activity should be looked at in 3 week mice to determine if pericyte loss is due to apoptosis. Assays that determine the activity of recruitment should be looked in 3 week mice to determine if this loss is due to lack of signaling, as other studies have shown that injections of PDGF-BB can cause abnormal modeling of the developing vasculature (Benjamin et al., 1998). Insulin levels play a big role in development of DR disease and the effects of insulin needs to be looked at to see if it has a role in pericyte cell death or signaling.

Although mouse models are good for early disease modeling in DR, they are not great models for late stage pathogenesis of DR. Retinal neovascularization, which does occur in humans, does not occur in mice unless induced through ischemia or having a specific targeted VEGF mutation (Grossniklaus et al., 2010). One reason could be due to mice are resistant to getting high blood pressure (hypertension) and formation of plaques in the arteries (atherogenesis) unless induced through targeted gene mutations (Breyer et al., 2004; Leong et al., 2015). Diabetic mouse models, like Akita and DB mice, lack renal failure that can be found in long-term diabetes (Breyer et al., 2004). Mouse models lack the clathrin heavy chain on chromosome 22 (CHC22) protein, which is important for glucose transport (Vassilopoulos et al., 2009). It is one or several of these differences in species why mouse models do not get the advanced stages of diabetes and DR, seen in humans. Further studies on DR and pericyte loos should be done on mouse models exhibiting both diabetes and one of the other factors, like renal failure or high blood pressure, to look at a better model for DR disease progression and more targets for drugs combating DR progression.

# REFERENCES

Agapova O.A, Kaufman P.L., Lucarelli M.J., Gabelt B.T., Hernandez M.R. Differential expression of matrix metalloproteinases in monkey eyes with experimental glaucoma or optic nerve transection. Brain Research, 2003; 967(1-2):132-143.

Akbar A. N., Lord J. M., and Salmon M. IFN-α and IFN-β: a link between immune memory and chronic inflammation. Immunology Today, 2000; 21(7):337-342.

Alao, J. P. The regulation of cyclin D1 degradation: roles in cancer development and the potential for therapeutic invention. Molecular Cancer, 2007; 6:24.

Allen T.J., Cooper M.E. and Lan H.Y. Use of genetic mouse models in the study of diabetic nephropathy. Current Diabetes Reports, 2004; 4:435-440.

American Diabetes Association, National Diabetes Statistics Report. 2017. http://www.diabetes.org/diabetes-basics/statistics

Back S. H. and Kaufman, R. J. Endoplasmic Reticulum Stress and Type 2 Diabetes. Annual Review of Biochemistry, 2012; 81:767–793.

Barber A.J., Antonetti D.A., Kern T.S., Reiter C.E.N., Soans R.S.,Krady J.K., Levison S.W., Gardner T.W., and Bronson S.K.. The Ins2Akita Mouse as a Model of Early Retinal Complications in Diabetes. Invest. Ophthalmol. Vis. Sci. 2005; 46(6):2210-2218.

Basu A.J. Involvement of protein kinase C-δ in DNA damage-induced apoptosis. J Cell Mol Med, 2003; 7:341-350.

Becher B., Tugues S., and Greter M. GM-CSF: From Growth Factor to Central Mediator of Tissue Inflammation. Immunity, 2016; 45(5):963-973.

Benjamin L. E., Hemo I., and Keshet, E. A plasticity window for blood vessel remodelling is defined by pericyte coverage of the preformed endothelial network and is regulated by PDGF-B and VEGF. Development, 1998; 125(9):1591-1598.

Ben-Neriah Y. and Karin M. Inflammation meets cancer, with NF-κB as the matchmaker. Nature Immunology, 2011; 12:715.

Bergers G. and Song S. The role of pericytes in blood-vessel formation and maintenance. Neuro-Oncology, 2005; 7(4):452-464.

Breyer M.D., Bottinger E., Brosius F.C., Coffman T.M., Harris R.C., Heilig C.W., Sharma K. Mouse models of diabetic nephropathy. Journal of American Society of Nephrology, 2004; 16:27–45.

Bringmann A., Pannicke T., Grosche J., Francke M., Wiedemann P., Skatchkov S.N., Osborne N.N., Reichenbach A. Müller cells in the healthy and diseased retina. Progress in Retinal and Eye Research, 2006; 25(4):397-424.

Brodie C. and Blumberg P.M. Regulation of cell apoptosis by protein kinase c δ Apoptosis, 2003; 8:19.

Brunet A., Datta S.R., and Greenberg M.E. Transcription-dependent and -independent control of neuronal survival by the PI3K–Akt signaling pathway. Current Opinion in Neurobiology, 2001; 11(3):297-305.

Burda J. E., and Sofroniew M. V. Reactive gliosis and the multicellular response to CNS damage and disease. Neuron, 2014; 81(2): 229–248.

Byeon S. H., Chung H. Y., and Kwon O. W. Polyunsaturated fatty acid composition of surgically removed hard exudates in diabetic macular edema. Ophthalmic Surg Lasers Imaging, 2010; 9:1-3.

C. Hsu J.-Y C., Bourguignon L.Y.W., Adams C.M., Peyrollier K., Zhang H., Fandel T., Cun C.L., Werb Z., Noble-Haeusslein L.J. Matrix Metalloproteinase-9 Facilitates Glial Scar Formation in the Injured Spinal Cord. Journal of Neuroscience, 2008; 28(50):13467-13477.

Cagnol S. and Chambard J. ERK and cell death: Mechanisms of ERK-induced cell death – apoptosis, autophagy and senescence. The FEBS Journal, 2010; 277:2-21.

Campbell I.A., Leong D., Edwards K.M., Rayzman V., Ng M., Goldberg G.L., Wilson N.J., Scalzo-Inguanti K., Mackenzie-Kludas C., Lawlor K.E., Wicks I.P., Brown L.E., Baz-Morelli A., Panousis C., Wilson M.J., Nash A.D., McKenzie B.S., and Andrews A.A. Therapeutic Targeting of the G-CSF Receptor Reduces Neutrophil Trafficking and Joint Inflammation in Antibody-Mediated Inflammatory Arthritis. Journal of Immunology, 2016; 197(11):4392-4402.

Cao, Y. Multifarious functions of PDGFs and PDGFRs in tumor growth and metastasis. Trends in Molecular Medicine, 2013; 19(8):460-473.

Centers for Disease Control and Prevention. National diabetes fact sheet: national estimates and general information on diabetes and prediabetes in the United States. 2011.

Chaudhary L. R. and Hruska K. A. The cell survival signal Akt is differentially activated by PDGF-BB, EGF, and FGF-2 in osteoblastic cells. Journal Cellular Biochemistry, 2001; 81:304-311.

Cheung A. K., Fung M. K., Lo A. C., Lam T. T., So K. F., Chung S. S., and Chung S. K. Aldose reductase deficiency prevents diabetes-induced blood-retinal barrier breakdown, apoptosis, and glial reactivation in the retina of db/db mice. Diabetes, 2005; 54:3119–3125.

Cheung N., Mitchell P., Wong T. Y. Diabetic retinopathy. Lancet, 2010; 376:124–136.

Chibber R., Molinatti PA., Rosatto N., Lambourne B., Kohner EM. Toxic action of advanced glycation end products on cultured retinal capillary pericytes and endothelial cells: relevance to diabetic retinopathy. Diabetologia, 1997; 40:156–164.

Chiu I.M., Phatnani H., Kuligowski M., Tapia J.C., Carrasco M.A., Zhang M., Maniatis T., Carroll M.C. Activation of innate and humoral immunity in the peripheral nervous system of ALS transgenic mice. Proceedings of the National Academy of Sciences, 2009; 106(49).

Chou J.C., Rollins S.D., Ye M., Batlle D., and Fawzi A.A. Endothelin Receptor-A Antagonist Attenuates Retinal Vascular and Neuroretinal Pathology in Diabetic Mice. Investigative Ophthalmology & Visual Science, 2014; 55(4):2516-2525.

Clements R. S., Robinson W. G., Cohen M. P. Anti-glycated albumin therapy ameliorates early retinal microvascular pathology in db/db mice. J. Diabetes Complications, 1998; 12(28):3.

Coleman DL. Obese and diabetes: two mutant genes causing diabetes-obesity syndromes in mice. Diabetologia, 1978; 14(3):141-8.

Coutinho I., Pereira G., Leão M., Gonçalves J., Côrte-Real M., and Saraiva L. Differential regulation of p53 function by protein kinase C isoforms revealed by a yeast cell system. FEBS Letters, 2009; 583.

Cunha-Vaz J., Rui B., and Conceição L. Blood-Retinal Barrier. European Journal of Ophthalmology, 2011; 21(6):3-9.

Curtis T. M., Gardiner T. A., Stitt A. W. Microvascular lesions of diabetic retinopathy: clues towards understanding pathogenesis. Eye, 2009; 23:1496–1508

Dandona P., Aljada A., and Bandyopadhyay A. Inflammation: the link between insulin resistance, obesity and diabetes. Trends in Immunology, 2004; 25(1):4-7.

De Hoz R., Rojas B., Ramírez A. I., Salazar J. J., Gallego B. I., Triviño A., and Ramírez J. M. Retinal Macroglial Responses in Health and Disease. BioMed Research International, 2016; 2016:2954721.

Deb D.K., Sassano A., Lekmine F., Majchrzak B., Verma A., Kambhampati S., Uddin S., Rahman A., Fish E.N., and Platanias K. Activation of Protein Kinase Cδ by IFN-γ. The Journal of Immunology, 2003; 171(1):267-273.

Derouiche A. and Rauen T. Coincidence of L-glutamate/L-aspartate transporter (GLAST) and glutamine synthetase (GS) immunoreactions in retinal glia: Evidence for coupling of GLAST and GS in transmitter clearance. Journal of Neuroscience, 1995; 42:131-143.

Deuse T., Koyanagi T., Erben R.G., Hua X., Velden J., Ikeno F., Reichenspurner H., Robbins R.C., Mochly-Rosen D., and Schrepfer S. Sustained Inhibition of ε Protein Kinase C Inhibits Vascular Restenosis After Balloon Injury and Stenting Circulation. 2010; 122:S170-S178.

Dharmarajan S., Fisk D. L., Sorenson C. M., Sheibani N., and Belecky-Adams T. L. Microglia activation is essential for BMP7-mediated retinal reactive gliosis. Journal of Neuroinflammation, 2017; 14(1):76.

Diehl N., and Schaal H. Make Yourself at Home: Viral Hijacking of the PI3K/Akt Signaling Pathway. Viruses, 2013; 5(12):3192–3212.

Drummond G. R., Selemidis S., Griendling K. K., and Sobey C. G. Combating oxidative stress in vascular disease: NADPH oxidases as therapeutic targets. Nature Reviews, 2011; 10(6):453–471.

Du Y., Sarthy V., and Kern T. Interaction between NO and COX pathways in retinal cells exposed to elevated glucose and retina of diabetic rats. American Journal Physiology, 2004; 287:R735-R741.

Dyer M. A., and Cepko C. L. Control of Müller glial cell proliferation and activation following retinal injury. Nature Neuroscience, 2000; 3:873.

Eizirik D. L., Colli M. L., and Ortis F. The role of inflammation in insulitis and β-cell loss in type 1 diabetes. Nature Reviews Endocrinology, 2009; 5:219.

Ellis P., Fagan B. M., Magness S. T., Hutton S., Taranova O., Hayashi S., McMahon A., Rao M., and Pevny L. SOX2, a Persistent Marker for Multipotential Neural Stem Cells Derived from Embryonic Stem Cells, the Embryo or the Adult. Dev Neurosci, 2004; 26:148-165.

Ernst C. and Christie B. R. Isolectin-IB4 as a vascular stain for the study of adult neurogenesis. Journal of Neuroscience Methods, 2006; 150(1):138-142.

Farrar M. A. and Schreiber, R. D. The Molecular Cell Biology of Interferon-gamma and its Receptor. Annual Review of Immunology, 1993; 11(1):571-611.

Feghali C.A. and Wright T.M. 12 Cytokines in Acute and Chronic Inflammation. Frontiers in Bioscience, 1997; 2:12-26.

Ferrero-Miliani L., Nielsen O. H., Andersen P. S., and Girardin S. E. Chronic inflammation: importance of NOD2 and NALP3 in interleukin-1β generation. Clinical and Experimental Immunology, 2007; 147(2):227–235.

Feuerer M., Eulenburg K, Loddenkemper C., Hamann A., and Huehn J. Self-limitation of Th1-mediated inflammation by IFN-gamma. Journal of Immunololgy. 2006; 176 (5):2857-63.

Fletcher E. L., Phipps J. A., Ward M. M., Puthussery T., and Wilkinson-Berka J. Neuronal and glial cell abnormality as predictors of progression of diabetic retinopathy. Current Pharmaceutical Design, 2007; 13(26):2699-712.

Frank R. N. Diabetic retinopathy. N. Engl. J. Med., 2004; 350:48–58.

Frantz C., Stewart K. M., and Weaver V. M. The extracellular matrix at a glance. Journal of Cell Science, 2010; 123(24):4195–4200.

Gabay C. and Kushner I. Acute-Phase Proteins and Other Systemic Responses to Inflammation. New England Journal of Medicine, 1999; 340(6):448-454.

Gabay C. Interleukin-6 and chronic inflammation. Arthritis Research and Therapy, 2006; 8(2):3.

Gao X., Zhang H., Takahashi T., Hsieh J., Liao J., Steinberg G. K., and Zhao H. The AKT signaling pathway contributes to postconditioning's protection against stroke; the protection is associated with the MAPK and PKC pathways. Journal of Neurochemistry, 2008; 105:943-955.

Gardner T.W., Antonetti D.A., Barber A. J., LaNoue K. F., Levison S.W. Diabetic Retinopathy. Survey of Ophthalmology, 2002; 47:S253-S262.

Geraldes P., and King G. L. Activation of Protein Kinase C Isoforms and Its Impact on Diabetic Complications. Circulation Research, 2010; 106(8):1319–1331.

Geraldes P., Hiraoka-Yamamoto J., Matsumoto M., Clermont A., Leitges M., Marette, A., Aiello L.P., Kern T.S., King, G. L Activation of PKCδ and SHP1 by hyperglycemia causes vascular cell apoptosis and diabetic retinopathy. Nature Medicine, 2009; 15(11):1298–1306.

Glaucoma Research Foundation, Eye Anatomy. 2017. http://www.glaucoma.org/anatomy-of-the-eye.php

Grigsby J.G., Cardona S.M., Pouw C.E., Muniz A., Mendiola A.S., Tsin A.T., Allen D.M., Cardona A.E. The Role of Microglia in Diabetic Retinopathy. Journal of Ophthalmology, 2014; 2014:705783.

Grossniklaus H.E., Kang S.J., and Berglin L. Animal Models of Choroidal and Retinal Neovascularization. Progress in retinal and eye research, 2010; 29(6):500-519.

Gumina R.J., Freire-Moar J., DeYoung L., Webb D.R., and Devens B.H. Transduction of the IFN-γ signal for HLA-DR expression in the promonocytic line THP-1 involves a late-acting PKC activity. Cellular Immunology, 1991; 138(2):265-279.

Hall P. A., Levison D. A., Woods A. L., Yu C. C., Kellock D. B., Watkins J. A., Barnes D.M., Gillett C.E., Camplejohn R., Dover R., Waseem N.H. and Lane, D. P. Proliferating cell nuclear antigen (PCNA) immunolocalization in paraffin sections: An index of cell proliferation with evidence of deregulated expression in some, neoplasms. J. Pathol., 1990; 162:285-294.

Hammes H.P., Lin J., Renner O., Shani M., Lundqvist A., Betsholtz C., Brownlee M., Deutsch U. Pericytes and the pathogenesis of diabetic retinopathy. Diabetes, 2002; 51:3107–3112.

Haurigot V., Villacampa P., Ribera A., Llombart C., Bosch A., Nacher V., Ramos D., Ayuso E., Segovia J., Bueren J.A., Ruberte J., and Bosch F. Increased Intraocular Insulin-like Growth Factor-I Triggers Blood-Retinal Barrier Breakdown J. Biol. Chem., 2009; 284: 22961.

Heinemann U., Kaufer D., and Friedman, A. Blood-brain barrier dysfunction, TGFβ signaling, and astrocyte dysfunction in epilepsy. Glia, 2012; 60:1251-1257

Hellstrom M., Gerhardt H., Kalen M., Li X., Eriksson U., Wolburg H., Betsholtz C. Lack of pericytes leads to endothelial hyperplasia and abnormal vascular morphogenesis. J Cell Biol, 2001; 153:543–554.

Hellstrom M., Kaln M., Lindahl P., Abramsson A., Betsholtz C. Role of PDGF-B and PDGFR-β in recruitment of vascular smooth muscle cells and pericytes during embryonic blood vessel formation in the mouse. Development, 1999; 126:3047–3055.

Hsieh C.L, Yang M.H, Chyau C.C, Chiu C.H, Wang H.E, Lin Y.C, Chiu W.T, Peng RY. Kinetic analysis on the sensitivity of glucose- or glyoxal-induced LDL glycation to the inhibitory effect of Psidium guajava extract in a physiomimic system. Biosystems, 2007; 88(1-2):92-100.

Ito D., Imai Y., Ohsawa K., Nakajima K., Fukuuchi Y., and Kohsaka S. Microglia-specific localisation of a novel calcium binding protein, Iba1. Molecular Brain Research, 1998; 57(1):1-9.

Jackson J.R., Seed M.P., Kircher C.H., Willoughby D.A., and Winkler J.D. The codependence of angiogenesis and chronic inflammation. The FASEB Journal, 1997; 11(6):457-465,

Jansson D., Scotter E. L., Rustenhoven J., Coppieters N., Smyth L. C. D., Oldfield R. L., Bergin P.S., Mee E.W., Graham E..S., Faull R.L., and Dragunow, M. Interferon-γ blocks signalling through PDGFRβ in human brain pericytes. Journal of Neuroinflammation, 2016; 13:249.

Johnson G.L., Stuhlmiller T.J., Angus S.P., Zawistowski J.S., and Graves L.M. Molecular Pathways: Adaptive Kinome Reprogramming in Response to Targeted Inhibition of the BRAF–MEK–ERK Pathway. Cancer Res 2014; 20(10):2516-2522.

Joussen A.M., Poulaki V., Mitsiades N., Cai W.Y., Suzuma I., Pak J., Ju S.T., Rook S.L., Esser P., Misiades C.S., Kirchof B., Adamis A.P., and Aiello.L.P. Suppression of Fas-FasL-induced endothelial cell apoptosis prevents diabetic blood-retinal barrier breakdown in a model of streptozotocin-induced diabetes. Faseb Journal, 2003; 17:76-78.

Kalliolias G. D. and Ivashkiv L. B. TNF biology, pathogenic mechanisms and emerging therapeutic strategies. Rheumatology, 2016; 12(1):49-62.

Kaur C., Foulds W.S., and Ling E.A. Blood-retinal barrier in hypoxic ischaemic conditions: basic concepts, clinical features and management. Prog Retin Eye, 2008; 27:622-647.

Keyel P.A. How is inflammation initiated? Individual influences of IL-1, IL-18 and HMGB1. Cytokine, 2014; 69(1):136-145.

Kolch W. Meaningful relationships: the regulation of the Ras/Raf/MEK/ERK pathway by protein interactions. Biochemical Journal, 2000; 351(2):289-305.

Kowluru R.A. and Odenbach S. Role of interleukin-1beta in the development of retinopathy in rats: effect of antioxidants. Invest. Ophthalmol. Vis. Sci., 2004; 45:4161-4166.

Kowluru R.A., Zhong Q., and Kanwar M. Metabolic memory and diabetic retinopathy: role of inflammatory mediators in retinal pericytes. Exp. Eye Res., 2010; 90:617-623

Kränkel N., Adams V., Linke A., Gielen S., Erbs S., Lenk K., Schuler G., and Hambrecht R. Hyperglycemia Reduces Survival and Impairs Function of Circulating Blood-Derived Progenitor Cells. Arteriosclerosis, Thrombosis, and Vascular Biology, 2005; 25:698-703.

Kreutzberg G.W. Microglia: a sensor for pathological events in the CNS. Trends in Neurosciences, 1996; 19(8):312-318.

Langmann, T. Microglia activation in retinal degeneration. Journal of leukocyte biology, 2007; 81:1345-51.

Lassègue B., Clempus R.E. Vascular NAD(P)H oxidases: specific features, expression, and regulation. American Journal of Physiology-Regulatory Integrative and Comparative Physiology, 2003; 285(2):R277–R297.

Lee M.S. and Kim Y-J. Signaling Pathways Downstream of Pattern-Recognition Receptors and Their Cross Talk. An. Rev. of Biochemistry, 2007; 76(1):447-480

Leong X.-F., Ng C.Y., and Jaarin K. Animal Models in Cardiovascular Research: Hypertension and Atherosclerosis. BioMed Research International, 2015; 11.

Leveen P., Pekny M., Gebre-Medhin S., Swolin B., Larsson E., Betsholtz C. Mice deficient for PDGF B show renal, cardiovascular, and hematological abnormalities. Genes Dev, 1994; 8:1875–1887.

Li G., Tang J., Du Y., Lee C.A., and Kern T.S. Beneficial effects of RAGE-Ig fusion protein on early diabetic retinopathy and tactile allodynia. Molecular vision, 2011; 17:3156-65.

Li L., Sampat K., Hu N., Zakari J., and Yuspa S.H. Protein Kinase C Negatively Regulates Akt Activity and Modifies UVC-induced Apoptosis in Mouse Keratinocytes. Journal of Biology and Chemistry, 2006; 281:3237.

Li M.O., Wan Y.Y, Sanjabi S., Robertson A-K L., Flavell R.A. Transforming Growth Factor-β Regulation of Immune Responses. Annual Review of Immunology, 2006; 24(1): 99-146.

Lindahl P., Johansson B.R., Leveen P., Betsholtz C. Pericyte loss and microaneurysm formation in PDGF-B-deficient mice. Science, 1997; 277:242–245.

Liu X., He Y., Li F., Huang Q., Kato T.A., Hall R.P., and Li C-Y. Caspase-3 Promotes Genetic Instability and Carcinogenesis. Molecular Cell, 2015; 58(2):284-296

Liwnicz B.H., Leach J.L. Yeh H-S, and Privitera M. Pericyte Degeneration and Thickening of Basement Membranes of Cerebral Microvessels in Complex Partial Seizures: Electron Microscopic Study of Surgically Removed Tissue. Neurosurgery, 1990; 26(3):409–420.

Lodeiro M., Alén B. O., Mosteiro C. S., Beiroa D., Nogueiras R., Theodoropoulou M., Pardo M., Gallego r., Pazos Y., Casaneuva F., and Camiña, J. P. The SHP-1 protein tyrosine phosphatase negatively modulates Akt signaling in the ghrelin/GHSR1a system. Molecular Biology of the Cell, 2011; 22(21):4182–4191.

Lodish H., Berk A., Zipursky S.L., Matsudaira P., Baltimore D., and Darnell J. Intermediate Filaments. Molecular Cell Biology, 2000; 19:6.

Lopez-Dee Z., Pidcock K., and Gutierrez L.S. Thrombospondin-1: Multiple Paths to Inflammation. Mediators of Inflammation, 2011; 2011.

Malavez Y., Gonzalez-Mejia M.E. and Doseff A.I. PRKCD (protein kinase C, delta) Atlas Genet Cytogenet Oncol Haematol, 2009; 13(1):28-42.

Margarkis N.J., Rothstein J.J. Mechanisms of disease: astroycites in neurodegenerative disease. Nat Clin Pract Neurol., 2006; 2(12):679-89.

Marques R.M., Guabiraba R., Russo R.C. and Teixeira M.M. Targeting CCL5 in inflammation. Expert Opinion on Therapeutic Targets, 2013; 17(12):1439-1460.

Midena E., Segato T., Radin S., di Giorgio G., Meneghini F., Piermarocchi S., and Belloni A. S. Studies on the retina of the diabetic db/db mouse. I. Endothelial cell-pericyte ratio. Ophthalmic Res., 1989; 21:106–111.

Nass N., Vogel K., Hofmann B., Presek P., Silber R.E., Simm A. Glycation of PDGF results in decreased biological activity. The International Journal of Biochemistry and Cell Biology, 2010; 42(5):749-754.

Nicholson T.M. and Anderson N.G. The protein kinase B/Akt signalling pathway in human malignancy. Cellular Signaling, 2002; 14(5):381-395.

Oates PJ. The polyol pathway and diabetic peripheral neuropathy. Neurobiology of Diabetic Neuropathy, 2002; 50:325–392.

Oever I.A.M., Raterman H. G., Nurmohamed M.T., and Simsek S. Endothelial Dysfunction, Inflammation, and Apoptosis in Diabetes Mellitus. Mediators of Inflammation, 2010; 2010:792393.

Oh J.-I., Chun K.-H., Jo, S.-H., Oh Y.-T., and Lee S.-K. Caspase-3-dependent protein kinase C delta activity is required for the progression of Ginsenoside-Rh2-induced apoptosis in SK-HEP-1 cells. Cancer Letters, 2005; 230(2):228–238.

Ozerdem U., Grako K. A., Dahlin-Huppe K., Monosov E. and Stallcup W. B. NG2 proteoglycan is expressed exclusively by mural cells during vascular morphogenesis. Dev. Dyn., 2011; 222: 218-227.

Pasha S., Münch S. P. B., Schäfer R., Oertel P., Sykes P., Zhu A.M. and Karl, M. O. Retinal cell death dependent reactive proliferative gliosis in the mouse retina. Scientific Reports, 2017; 7(1):9517.

Pekny M. and Nilsson M. Astrocyte activation and reactive gliosis. Glia, 2005; 50(4):427-34.

Pfaffl, M. W. A new mathematical model for relative quantification in real-time RT–PCR. Nucleic Acids Research, 2001; 29(9):e45.

Porter A. G., and Jänicke R. U. Emerging roles of caspase-3 in apoptosis. Cell Death and Differentiation, 1999; 6:99.

Powell E.D. and Field R.A. Diabetic retinopathy and rheumatoid arthritis. Lancet, 1964; 2:17-18.

Purves D., Augustine G.J., and Fitzpatrick D. The Retina. Neuroscience, 2001.

Rawlings J.S., Rosler K.M., and Harrison D.A. The JAK/STAT signaling pathway. Journal of Cell Science, 2004; 117:1281-1283.

Ridet J.L., Privat A., Malhotra S.K., and Gage F.H. Reactive astrocytes: cellular and molecular cues to biological function. Trends in Neurosciences, 1997; 20(12): 570-577.

Robinson, R., Barathi, V. A., Chaurasia, S. S., Wong, T. Y., and Kern, T. S. Update on animal models of diabetic retinopathy: from molecular approaches to mice and higher mammals. Disease Models and Mechanisms, 2012; 5(4):444–456.

Romeo G., Liu W-H, Asnaghi V., Kern T.S., and Lorenzi M. Activation of Nuclear Factor-κB Induced by Diabetes and High Glucose Regulates a Proapoptotic Program in Retinal Pericytes. Diabetes, 2002; 51(7):2241-2248.

Roque R. S. and Caldwell R. B. Müller cell changes precede vascularization of the pigment epithelium in the dystrophic rat retina. Glia, 1990; 3:464-475.

Saaddine J.B., Honeycutt A., Narayan K., Zhang X., Klein R., Boyle J. Projection of Diabetic Retinopathy and Other Major Eye Diseases Among People With Diabetes Mellitus. Arch Ophthalmol, 2008; 126(12):1740–1747.

Sataranatarajan K., Ikeno Y., Bokov A., Feliers D., Yalamanchili H., Lee H.J., Mariappan M.M., Tabatabai-Mir H., Diaz V., Prasad S., Javor M.A., Ghosh C.G., Hubbard G.B., Barnes J.L., Richardson A., and S. Kasinath B.S. Rapamycin Increases Mortality in db/db Mice, a Mouse Model of Type 2 Diabetes. The Journals of Gerontology, 2016; 71(7):850–857.

Scheller J., Chalaris A., Schmidt-Arras D., and Rose-John S. The pro- and anti-inflammatory properties of the cytokine interleukin-6. Molecular Cell Research, 2011; 1813(5):878-888.

Schneider C. A., Rasband W. S. and Eliceiri, K. W. NIH Image to ImageJ: 25 years of image analysis. Nature methods, 2012; 9(7):671-675.

Selmaj K.W., Farooq M., Norton W.T., Raine C.S., and Brosnan C.F. Proliferation of astrocytes in vitro in response to cytokines. A primary role for tumor necrosis factor. The Journal of Immunology, 1990; 144(1):129-135.

Seok J., Warren H. S., Cuenca A. G., Mindrinos M.N., Baker H.V., Xu W., Richards D.R., McDonald-Smith G.P., Gao H., Hennessy L., Finnerty C.C., Lopez C.M., Honari S., Moore E.E., Minei J.P., Cuschieri J., Bankey P.E., Johnson J.L., Sperry J., Nathen A.B., Billiar T.R., West M.A., Jeschke M.G., Klein M.B., Gamelli R.L., Gibran N.S., Brownstein B.H., Miller-Graziano C., Calvana S.E., Mason P.H., Cobb J.P., Rahme L.G., Lowry S.F., Maier R.V., Moldawer L.L., Herndon D.N., Davis R.W., Xiao W., and Tompkins, R.G. Genomic responses in mouse models poorly mimic human inflammatory diseases. Proceedings of the National Academy of Sciences, 2013; 110(9):3507-3512.

Sharma K., McCue P. and Dunn S.R. Diabetic kidney disease in the db/db mice. American Journal of Physiology-Renal Physiology, 2003; 284:F1138-F1144.

Shaul Y.D. and Seger R. The MEK/ERK cascade: From signaling specificity to diverse functions. Molecular Cell Research, 2007; 1773(8):1213-1226.

Shen S., Yu S., Binek J., Chalimoniuk M., Zhang X., Lo S.C., Hannick M., Wu J., Fritsche K., Donato R., and Sun G.Y. Distinct signaling pathways for induction of type II NOS by IFNγ and LPS in BV-2 microglial cells. Neurochemistry International, 2005; 47(4):298-307.

Shin E. S., Sorenson C. M., and Sheibani N. Diabetes and Retinal Vascular Dysfunction. Journal of Ophthalmic and Vision Research, 2014; 9(3):362–373.

Silver J., and Mille, J. H. Regeneration beyond the glial scar. Neuroscience, 2004; 5:146.

Singh V. K., Mehrotra S., and Agarwal S. S. The paradigm of Th1 and Th2 cytokines. Immunologic Research, 1999; 20(3):147-161.

Singh V. P., Bali A., Singh N., and Jaggi A. S. Advanced Glycation End Products and Diabetic Complications. The Korean Journal of Physiology and Pharmacology, 2014; 18(1):1–14.

Sofroniew M.V. Molecular dissection of reactive astrogliosis and glial scar formation. Trends in Neurosciences, 2009; 32(12):638-647.

Stieinberg S.F. Distinctive activation mechanisms and functions for protein kinase Cδ. Biochem J, 2004; 384:449-459.

Stitt A.W., Hughes S.J., Canning P., Lynch O., Cox O., Frizzell N., Thorpe S.R., Cotter T.G., Curtis T.M., Gardiner T.A. Substrates modified by advanced glycation end-products cause dysfunction and death in retinal pericytes by reducing survival signals mediated by platelet-derived growth factor. Diabetologia, 2004; 47:1735–1746.

Streit W.J., Walter S.A., Pennell N.A. Reactive microgliosis. Progress in Neurobiology, 1999; 57(6):563-581.

Swain S. L. T Cell Subsets and the Recognition of MHC Class. Immunological Reviews, 1983; 74:129-142.

Sweeney M. D., Ayyadurai S., and Zlokovic, B. V. Pericytes of the neurovascular unit: Key functions and signaling pathways. Nature Neuroscience, 2016; 19(6):771–783.

Szwergold B.S., Kappler F., Brown T.R. Identification of fructose 3-phosphate in the lens of diabetic rats. Science, 1990; 247(4941):451–454.

Tadayoni R., Paques M., Gaudric A., and Vicaut E. Erythrocyte and leukocyte dynamics in the retinal capillaries of diabetic mice. Exp. Eye Res., 2003; 77:497–504.

Tanaka Y., Gavrielides M.V., Mitsuuchi Y., Fujii T., and Kazanietz M.G. Protein Kinase C Promotes Apoptosis in LNCaP Prostate Cancer Cells through Activation of p38 MAPK and Inhibition of the Akt Survival Pathway J. Biol. Chem., 2003; 278: 33753.

Tang J., and Kern T. S. Inflammation in diabetic retinopathy. Progress in Retinal and Eye Research, 2011; 30(5):343-358.

Taniguchi T., Ogasawara K., Takaoka A., and Tanaka N. IRF Family of Transcription Factors as Regulators of Host Defense. Annual Review of Immunology, 2001; 19(1):623-655.

Tilg H., Trehu E.G., Atkins M.B., Dinarello C.A., and Mier J.W. Interleukin-6 (IL-6) as an anti-inflammatory cytokine: induction of circulating IL-1 receptor antagonist and soluble tumor necrosis factor receptor p55. Blood, 1994; 83(1):113-118.

Treisman R. Regulation of transcription by MAP kinase cascades. Current Opinion in Cell Biology, 1996; 8(2):205-215.

Uddin S., Sassano A., Deb D.K., Verma A., Majchrzak B., Rahman A., Malik A., Fish E.N., and Platanias L.C. Protein Kinase C-δ (PKC-δ) Is Activated by Type I Interferons and Mediates Phosphorylation of Stat1 on Serine 727. J. Biol. Chem., 2002; 277:14408.

Ueno, Y., Horio, F., Uchida, K., Naito, M., Nomura, H., Kato, Y., Tsuda, T., Toyokuni, S. and Osawa, T. Increase in oxidative stress in kidneys of diabetic Akita mice. Bioscience, Biotechnology, and Biochemistry, 2002; 66:869-872

Vassilopoulos S., Esk C., Hoshino S., Funke B., Chen C.-Y., Plocik A.M., Wright W., Kucherlapati R., and Brodsky F.M. A Role for the CHC22 Clathrin Heavy Chain Isoform in Human Glucose Metabolism. Science, 2009; 324(5931):1192-1196.

Vezzani A. and Granata T. Brain Inflammation in Epilepsy: Experimental and Clinical Evidence. Epilepsia, 2005; 46:1724-1743.

Villacampa P., Ribera A., Motas S., Ramírez L., García M., de la Villa P., Haurigot V., and Bosch F. Insulin-like Growth Factor I (IGF-I)-induced Chronic Gliosis and Retinal Stress Lead to Neurodegeneration in a Mouse Model of Retinopathy J. Biol. Chem., 2013; 288:17631.

Villarroel M., Ciudin A., Hernández C., Simo R. Neurodegeneration: An early event of diabetic retinopathy. World J. Diabetes, 2010; 15:57–64.

Wang J, Takeuchi T, Tanaka S, Kubo S.K., Kayo T., Lu D., Takata K., Koizumi A., and Izumi T. A mutation in the insulin 2 gene induces diabetes with severe pancreatic beta-cell dysfunction in the Mody mouse. J Clin Invest, 1999; 103:27–37.

Wasim, M., Awan, F.R., Najam, S.S., Khan A.R., and Khan H.N. Role of Leptin Deficiency, Inefficiency, and Leptin Receptors in Obesity. Biochem Genet, 2016; 54:565.

Wellen K.E. and Hotamisligil G.S. Inflammation, stress, and diabetes. J Clin Invest. 2005; 115(5):1111-1119.

Wilkinson C., Ferris F. L. III, Klein R. E., Lee P. P., Agardh C. D., Davis M., Dills D., Kampik A., Pararajasegaram R., and Verdaguer J. T. Proposed international clinical diabetic retinopathy and diabetic macular edema disease severity scales. Ophthalmology, 2003; 110(9):1677–1682.

Williams K.A., Zhanga M., Xianga S., Chen H., Wua J.Y., Zhang S., Ryan M., Cox A.D., Channing J. D., Fang B., Koomen J., Haurag E., Beplerh G., Nicosia S.V., Matthiasi P., Wang C., Bai W., and Zhanga X. Extracellular Signal-regulated Kinase (ERK) Phosphorylates Histone Deacetylase 6 (HDAC6) at Serine 1035 to Stimulate Cell Migration. JBC, 2013; 288(46):33156-70.

World Health Organization, Global report on diabetes. 2017. http://www.who.int/diabetes/global-report/en

Wright W.S., Yadav A.S., McElhatten R.M., and Harris N.R. Retinal blood flow abnormalities following six months of hyperglycemia in the Ins2(Akita) mouse. Experimental Eye Research, 2012; 98:9-15.

Yang Q., Xu Y., Xie P., Cheng H., Song Q., Su T., Yuan S., and Liu Q. Retinal Neurodegeneration in db/db Mice at the Early Period of Diabetes. Journal of Ophthalmology, 2015; 2015:757412.

Yau, J. W. Y., Rogers, S. L., Kawasaki, R., Lamoureux, E. L., Kowalski, J. W., Bek, T., Chen S.J., Dekker J.M., Fletcher A., Grauslund J., Haffner S., Hamman R.F., Ikram M.K., Kayama T., Klein r., Krishnaiah S., Mayura K., O'Hare J.P., Orchard T.J., Porta M., Rema M., Roy M.S., Sharma T., Shaw J., Taylor H., Tielsch J.M., Varma R., Wang J.J., Wang N., West S., Xu L., Yasuda M., Zhang X., Mitchell P., Zhang x., Mitchell P., and Wong T.Y. Global Prevalence and Major Risk Factors of Diabetic Retinopathy. Diabetes Care, 2012; 35(3):556–564.

Yoshioka M., Kayo T., Ikeda T., and Koizuni A. A Novel Locus, Mody4, Distal to D7Mit189 on Chromosome 7 Determines Early-Onset NIDDM in Nonobese C57BL/6 (Akita) Mutant Mice. Diabetes, 1997; 46(5):887-894.

Zamanian J.L., Xu L., Foo L.C., Nouri N., Zhou L., Giffard R.G., and Barres B.A. Genomic Analysis of Reactive Astrogliosis. Journal of Neuroscience, 2012; 32(18):6391-6410.

Zarogoulidis P., Lampaki S., Turner J. F., Huang H., Kakolyris S., Syrigos K., and Zarogoulidis K. mTOR pathway: A current, up-to-date mini-review. Oncology Letters, 2014; 8(6):2367–2370.

Zeng H., Green W.R., Tso M.O.M. Microglial Activation in Human Diabetic Retinopathy. Arch Ophthalmol, 2008; 126(2):227–232.

Zittermann S. I. and Issekutz, A. C. Endothelial growth factors VEGF and bFGF differentially enhance monocyte and neutrophil recruitment to inflammation. Journal of Leukocyte Biology, 2006; 80:247-257.

Zongchao H., Guo J., Conley S.M., and Naash M. I. Retinal Angiogenesis in the Ins2Akita Mouse Model of Diabetic Retinopathy. Invest. Ophthalmol. Vis. Sci. 2013; 54(1):574-584.

Zudaire E., Gambardella L., Kurcz C., and Vermeren S. A Computational Tool for Quantitative Analysis of Vascular Networks. PLOS ONE, 2011; 6(11):27385.

# VITA

**Shukun Wang**

**Education**

- Masters of Biology at Purdue University
- Bachelors of Science at Indiana University Bloomington

**Training Experience**

- RT-qPCR, Mammalian Cell Culture, Immunoflourescence, Western Blotting, Mouse Colony Maintenance, Genotyping, Intra-vitreal Injections

**Professional Experience**

- Teaching Assistance 08/2016 – 05/2018
    - Immunology Laboratory – K339
- Research Assistance 07/2016 - 08/2018

**Conferences Attended**

- Third Annual Diabetes Symposium - Comparative Analysis of Retinal Glia and Cells of the Vasculature in Two Diabetic Mouse Models.
- Greater Indiana Society for Neuroscience - Comparative Analysis of Retinal Glia and Cells of the Vasculature in Two Diabetic Mouse Models.

**Publications**

- Inflammation in Type 1 and Type 2 mouse models of diabetic retinopathy. In review